National Center for Theoretical Sciences

A kinetic model for a polyatomic gas with temperature-dependent specific heats and its application to shock-wave structure

NCTS/Math
Technical Report
2019-002

Shingo Kosuge
Hung-Wen Kuo
Kazuo Aoki

Noname manuscript No.
(will be inserted by the editor)

Shingo Kosuge[1] · **Hung-Wen Kuo**[2] ·
Kazuo Aoki[2,3]

A kinetic model for a polyatomic gas with temperature-dependent specific heats and its application to shock-wave structure

February 28, 2019

Abstract The ellipsoidal statistical (ES) model of the Boltzmann equation for a polyatomic gas, proposed by Andries *et al.* [P. Andries et al., Eur. J. Mech. B/Fluids **19**, 813 (2000)], is extended to a polyatomic gas with temperature-dependent specific heats (thermally perfect gas). Then, the new model equation is used to investigate the structure of a plane shock wave with special interest in CO_2 gas, which is known to have a very large bulk viscosity, and in the case of relatively strong shock waves. The numerical and asymptotic analyses are performed in parallel to the previous paper by two of the present authors [S. Kosuge and K. Aoki, Phys. Rev. Fluids **3**, 023401 (2018)], where the structure of a shock wave in CO_2 gas was investigated using the ES model for a polyatomic gas with constant specific heats (calorically perfect gas). From the numerical and analytical results, the effect of temperature-dependent specific heats is clarified.

Keywords Boltzmann equation · ellipsoidal statistical model · polyatomic gas · temperature-dependent specific heats · shock-wave structure

1 Introduction

In recent years, the study of nonequilibrium polyatomic gas flows based on kinetic theory becomes increasingly important in various applications involving high-temperature circumstances [36, 38, 30, 12]. However, the original Boltzmann equation for a polyatomic gas is usually presented in rather abstract forms [17, 16, 29, 9], so that it is not possible to apply it immediately to practical problems. Therefore, some simplified and tractable models for collision integrals involving

Shingo Kosuge
E-mail: kosuge.shingo.6r@kyoto-u.ac.jp

[1]Institute for Liberal Arts and Sciences, Kyoto University, Kyoto 606-8501, Japan
[2]Department of Mathematics, National Cheng Kung University, Tainan 70101, Taiwan
[3]National Center for Theoretical Sciences, National Taiwan University, Taipei 10617, Taiwan

the energy transfer between the translational and internal modes have been proposed. One approach is to model the collision terms partially in the level of the original Boltzmann equation [11,43,19], while the other is to replace the entire collision terms by simpler models of the Bhatnagar–Gross–Krook (BGK) type [37,55,49,41,10,3,4,9,7], of the Fokker–Planck type [13,21,35], of the type of ellipsoidal statistical (ES) model [25,2], and of other types [23,46,42,39]. Some of the models in the latter category, which we call *model Boltzmann equations*, have been applied to fundamental problems in kinetic theory, such as the velocity-slip and temperature-jump problems [32,34,47,24].

One of the recent examples of the application of the model Boltzmann equations is the study of the structure of a plane shock wave in a polyatomic gas using the ES model, which was proposed in [2] and rederived in a systematic way in [14], with special interest in gases with large bulk viscosity [28,27]. The study was motivated by interesting results based on the extended thermodynamics that made a classification of the profile of a plane shock wave in carbon dioxide (CO_2) gas [51,52,45,53]. In [27], a direct numerical analysis using the ES model was carried out, and the result of this kinetic approach showed good agreement with the result in [52] obtained by the macroscopic approach (see also [54]).

The ES model used in [28,27] is constructed for a gas in which the specific heat at constant volume C_v and that at constant pressure C_p are constants. Such an ideal gas is called *calorically perfect* gas [31] (it is also called a *polytropic* gas in the literature). However, according to the literature, C_v, C_p, and thus the ratio of the specific heats $\gamma = C_p/C_v$ generally depend on the temperature. For instance, $\gamma \approx 1.3$ at 290K and $\gamma \approx 1.18$ at 1000K for CO_2 gas. Therefore, in [27], γ was set to be a constant according to the overall behavior of CO_2 gas. There seemed to be no problem for a weak shock in which the temperature variation across the shock is not large. However, for a strong shock, where the temperature variation is large, one cannot expect the correct behavior from the model with a constant γ. Therefore, as the continuation of the previous work [28,27], we have decided to investigate the same problem, i.e., the structure of a plane shock wave (for CO_2 gas), using a model Boltzmann equation that allows the temperature dependence of C_v, C_p, and thus γ. Incidentally, an ideal gas with temperature-dependent C_v, C_p and γ is called *thermally perfect* gas [31] (it is also called a *non-polytropic* gas in the literature).

Several model Boltzmann equations for a gas with temperature-dependent C_v and C_p have been proposed, such as the models proposed in [49,42,10,3,4,7], and we can utilize one of them for the present purpose. In [28,27], a careful numerical analysis, based on the ES model, was carried out. In addition, a systematic asymptotic analysis has been performed for large bulk viscosity to describe the slow relaxation of the internal modes inside a shock wave in CO_2 gas. In fact, the asymptotic analysis led to a system of ordinary differential equations for macroscopic quantities that can be solved analytically, and the resulting solution described the slow relaxation very well. In the present study, we are aiming at reproducing these results for CO_2 gas in the case where the specific heats are temperature dependent. However, if we use a model Boltzmann equation whose structure is completely different from the ES model, we expect to encounter difficulties in the analysis, comparison, and interpretation. For this reason, we have decided to extend the ES model in [2] to the case of temperature-dependent specific heats first and then apply the resulting model Boltzmann equation to the problem of the shock-wave structure.

The paper is organized as follows. After this introduction, we propose a new ES model for a polyatomic gas with temperature-dependent specific heats in Sect. 2.1 and summarize its basic properties and transport coefficients in Sects. 2.2 and 2.3, making occasional use of Appendices. Section 3 is devoted to the study of the structure of a shock wave on the basis of the model proposed in Sect. 2.1. To be more specific, the problem is formulated and reduced in Sects. 3.1–3.4, and numerical analysis is performed in Sects. 3.5 and 3.6. In Sect. 3.7, we summarize the result of the asymptotic analysis for large bulk viscosity. A short concluding remarks are given in Sect. 4.

2 Model equation and its basic properties

In the present section, we will propose a new kinetic model for an ideal polyatomic gas with temperature-dependent specific heats. Our starting point is the ES model proposed in [2] for a polyatomic gas with constant specific heats. However, we adopt a different representation from the original one in [2], that is, we take the ES model in the form used in [50, 24] as our starting point. The difference between these two representations will be discussed at the end of Sect. 2.1.

2.1 Model equation

Let us consider a polyatomic rarefied gas. Let t be the time variable, $\boldsymbol{X}$ (or X_i) the position vector in the physical space, $\boldsymbol{\xi}$ (or ξ_i) the molecular velocity, and $\mathscr{E}$ the energy associated with the internal modes per unit mass. We denote the number of the gas molecules contained in an infinitesimal volume $d\boldsymbol{X}d\boldsymbol{\xi}d\mathscr{E}$ around a point $(\boldsymbol{X}, \boldsymbol{\xi}, \mathscr{E})$ in the seven-dimensional space consisting of $\boldsymbol{X}$, $\boldsymbol{\xi}$, and $\mathscr{E}$ at time t by

$$\frac{1}{m} f(t, \boldsymbol{X}, \boldsymbol{\xi}, \mathscr{E}) d\boldsymbol{X} d\boldsymbol{\xi} d\mathscr{E}, \tag{1}$$

where m is the mass of a molecule. We call $f(t, \boldsymbol{X}, \boldsymbol{\xi}, \mathscr{E})$ the velocity/energy distribution function of the gas molecules.

In the present study, we consider the thermally perfect gas (or non-polytropic gas), for which the specific heat at constant volume C_v and that at constant pressure C_p are both functions of the temperature T. We will propose a model Boltzmann equation for such a gas, which is an extension of the ES model ([2, 14]) expressed in the form used in [50, 24].

Let us consider a system containing a gas at an equilibrium state at rest at temperature T. If we consider the case where C_v is constant, denote by D the internal degrees of freedom of the gas, and assume the equipartition law, then the internal energy of the gas per unit mass $E(T)$ is expressed as

$$E(T) = (3 + D)RT/2, \tag{2}$$

where R is the gas constant per unit mass, i.e., $R = k/m$ with k being the Boltzmann constant. In this case, $C_v = (3 + D)R/2$.

Next, we consider the case where C_v depends on the temperature. Let us suppose that C_v in the equilibrium state is a given function $C_v(T)$ of T that satisfies $C_v(T) > 3R/2$. Then, the internal energy $E(T)$ in this state is expressed as

$$E(T) = \int_{T_*}^{T} C_v(s)ds + E_*, \tag{3}$$

where T_* is the possible minimum temperature of the system and E_* is assumed to be $E_* > 3RT_*/2$. If the value of E is given as $E(T) = e$, then T is determined uniquely as $T = E^{-1}(e)$, where E^{-1} is the inverse function of E. In (2), $E(T)$ is defined in such a way that $E(0) = 0$. One way to keep consistency between (2) and (3) is to define E_* as $E_* = T_*C_v(T_*)$. Then, for T close to T_*, (3) becomes $E(T) = (T - T_*)C_v(T_*) + O(T - T_*) + T_*C_v(T_*) = TC_v(T_*) + O(T - T_*)$, which gives a consistent result $E(T_*) = T_*C_v(T_*)$.

Now, using the relation (2), we extend D as a continuous function of T defined by

$$D(T) = \frac{2}{RT}E(T) - 3, \tag{4}$$

for an arbitrarily given $E(T)$ [or $C_v(T)$]. Then, since $E(T) > 3RT/2$ for $T \geq T_*$, $D(T) > 0$ holds for $T \geq T_*$. To be consistent with (3), $D(T_*)$ should be $D(T_*) = 2E_*/RT_* - 3$.

Let us then consider the case where the gas is not in the equilibrium state. We extend $C_v(T)$, $E(T)$, $D(T)$, and the inverse function E^{-1} to the nonequilibrium case. In particular, when the internal energy is given as $E = e(t, \boldsymbol{X})$, where e is a given function of t and $\boldsymbol{X}$, we define the temperature $T(t, \boldsymbol{X})$ by $T = E^{-1}(e)$. Thus, $D(T)$ with this temperature $T(t, \boldsymbol{X})$ is an *extended* internal degrees of freedom in the nonequilibrium case. We further define the *extended* ratio of the specific heats $\gamma(T)$ as

$$\gamma(T) = \frac{C_p(T)}{C_v(T)} = \frac{C_v(T) + R}{C_v(T)}, \tag{5}$$

with the temperature $T(t, \boldsymbol{X})$, using the relation $C_p = C_v + R$. Since $C_v(T) > 3R/2$, $\gamma(T) < 5/3$ holds. With these preparations, we define our model Boltzmann equation in the following.

The velocity/energy distribution function of the gas molecules f is governed by the equation of the following form:

$$\frac{\partial f}{\partial t} + \xi_i \frac{\partial f}{\partial X_i} = Q(f), \tag{6}$$

with

$$Q(f) = A_c(T)\rho(\mathscr{G} - f). \tag{7}$$

Here,

$$\mathscr{G} = \frac{\rho \mathscr{E}^{\delta/2-1}}{(2\pi)^{3/2}[\det(\mathsf{T})]^{1/2}(RT_{\mathrm{rel}})^{\delta/2}\Gamma(\delta/2)} \times \exp\left(-\frac{1}{2}(\mathsf{T}^{-1})_{ij}(\xi_i - v_i)(\xi_j - v_j) - \frac{\mathscr{E}}{RT_{\mathrm{rel}}}\right), \tag{8a}$$

$$(\mathsf{T})_{ij} = (1-\theta)[(1-\nu)RT_{\rm tr}\delta_{ij} + \nu p_{ij}/\rho] + \theta RT\delta_{ij}, \tag{8b}$$

$$\rho = \iint_0^\infty f d\mathscr{E} d\boldsymbol{\xi}, \qquad v_i = \frac{1}{\rho}\iint_0^\infty \xi_i f d\mathscr{E} d\boldsymbol{\xi}, \tag{8c}$$

$$p_{ij} = \iint_0^\infty (\xi_i - v_i)(\xi_j - v_j) f d\mathscr{E} d\boldsymbol{\xi}, \tag{8d}$$

$$T = E^{-1}(e), \qquad \delta = D(T) = 2e/RT - 3, \tag{8e}$$

$$T_{\rm tr} = 2e_{\rm tr}/3R, \qquad T_{\rm int} = 2e_{\rm int}/R\delta, \qquad T_{\rm rel} = \theta T + (1-\theta)T_{\rm int}, \tag{8f}$$

where e, $e_{\rm tr}$, and $e_{\rm int}$ are defined by

$$e = e_{\rm tr} + e_{\rm int}, \qquad e_{\rm tr} = \frac{1}{2\rho}\iint_0^\infty |\boldsymbol{\xi} - \boldsymbol{v}|^2 f d\mathscr{E} d\boldsymbol{\xi}, \qquad e_{\rm int} = \frac{1}{\rho}\iint_0^\infty \mathscr{E} f d\mathscr{E} d\boldsymbol{\xi}. \tag{9}$$

In (7)–(9), ρ is the density, $\boldsymbol{v}$ (or v_i) is the flow velocity, p_{ij} is the stress tensor, e is the internal energy per unit mass, $e_{\rm tr}$ is that associated with the translational motion, $e_{\rm int}$ is that associated with the internal modes, T is the temperature, $T_{\rm tr}$ is the temperature associated with the translational motion, $T_{\rm int}$ is the temperature associated with the energy of the internal modes, $d\boldsymbol{\xi} = d\xi_1 d\xi_2 d\xi_3$, and the domain of integration with respect to $\boldsymbol{\xi}$ is the whole space of $\boldsymbol{\xi}$. The symbol δ_{ij} indicates the Kronecker delta, and $\nu \in [-1/2, 1)$ and $\theta \in [0, 1]$ are parameters, whose relation with the transport coefficients will be shown later [cf. (27)]. In addition, $A_c(T)$ is a function of T such that $A_c(T)\rho$ is the collision frequency of the gas molecules, $\Gamma(z)$ is the gamma function defined by

$$\Gamma(z) = \int_0^\infty s^{z-1} e^{-s} ds, \tag{10}$$

T is the 3×3 positive-definite symmetric matrix whose (i, j) component is defined by (8b), and $\det(\mathsf{T})$ and T^{-1} are, respectively, its determinant and inverse. Here and in what follows, we basically use the summation convention, i.e., $a_i b_i = \sum_{i=1}^3 a_i b_i$, $c_{ij} a_i b_j = \sum_{i,j=1}^3 c_{ij} a_i b_j$, etc.

Note that all the macroscopic quantities contained in $\mathscr{G}$ are generated from f. To be more specific, (i) ρ, $\boldsymbol{v}$, p_{ij}, $e_{\rm tr}$, $e_{\rm int}$, and e are obtained by (8c), (8d), and (9); (ii) T and then δ are determined by (8e) using the inverse function E^{-1} of the function E [cf. (3)]; (iii) $T_{\rm tr}$, $T_{\rm int}$, and $T_{\rm rel}$ are determined by (8f), and then T is established by (8b). Since $e = e_{\rm tr} + e_{\rm int} = (3T_{\rm tr} + \delta T_{\rm int})R/2$ and also $e = (3+\delta)RT/2$, we have the relation

$$T = \frac{3T_{\rm tr} + \delta T_{\rm int}}{3+\delta}. \tag{11}$$

The major difference of the present model from the original ES model is that δ is not a constant but is a function of the temperature T. Therefore, (11) gives an implicit relation for T, $T_{\rm tr}$, and $T_{\rm int}$. However, to avoid complexity of the notation, we just denote it by δ rather than $\delta(T)$ here and in what follows.

The pressure p and the heat-flow vector q_i are given by

$$p = R\rho T, \tag{12a}$$

$$q_i = \iint_0^\infty (\xi_i - v_i)\left(\frac{1}{2}|\boldsymbol{\xi} - \boldsymbol{v}|^2 + \mathscr{E}\right) f d\mathscr{E} d\boldsymbol{\xi}, \tag{12b}$$

where (12a) is the equation of state.

In [2], the case of $\theta = 0$ is excluded because the bulk viscosity becomes infinitely large in this case [cf. (27b)]. However, as shown in [27], the case of $\theta = 0$ plays an important role in describing the structure of a shock wave in a gas with large bulk viscosity. Therefore, we have included this case in the model (7) and let the admissible range of θ be $\theta \in [0, 1]$. In Sect. 2.2, the case of $\theta = 0$ will be treated separately.

In [2], the energy variable $\mathscr{E}$, which is denoted by ε there, is assumed to be expressed as $\mathscr{E} = I^{2/\delta}$ in terms of a variable I and a constant δ, and I is used as an independent variable (see [50]). To be more specific, the distribution function in [2], which is denoted by $f^{\mathrm{A}}(t, \boldsymbol{X}, \boldsymbol{\xi}, I)$ here, is defined in such a way that

$$\frac{1}{m} f^{\mathrm{A}}(t, \boldsymbol{X}, \boldsymbol{\xi}, I) d\boldsymbol{X} d\boldsymbol{\xi} dI, \tag{13}$$

indicates the number of the molecules with position in $d\boldsymbol{X}$ (around $\boldsymbol{X}$), velocity in $d\boldsymbol{\xi}$ (around $\boldsymbol{\xi}$), and the variable I in dI (around I) at time t. Therefore, the relation between f^{A} and our f is as follows:

$$f(t, \boldsymbol{X}, \boldsymbol{\xi}, \mathscr{E}) = (\delta/2)\mathscr{E}^{\delta/2-1} f^{\mathrm{A}}(t, \boldsymbol{X}, \boldsymbol{\xi}, \mathscr{E}^{\delta/2}). \tag{14}$$

In addition, Λ_δ in [2] is expressed as

$$\Lambda_\delta^{-1} = (\delta/2)\Gamma(\delta/2). \tag{15}$$

The representation of the ES model using $\mathscr{E}$ is equivalent to that using I as far as a polyatomic gas with constant specific heats is concerned. However, our new model (6), which is an extension based on the representation using $\mathscr{E}$, is, in general, different from a model obtained by a similar extension from the representation using I.

An extension of the BGK model to a gas with temperature-dependent specific heats, which is based on the $\mathscr{E}$-representation and is along the same line as the present work, has been proposed independently in [7]. On the other hand, a sophisticated extension of the BGK model using the I-representation for each of rotational energy and vibrational energy was proposed recently in [3,4].

2.2 Basic properties

In this subsection, we summarize some basic properties of the model proposed in Sect. 2.1. Here, we assume that $\theta \neq 0$. The case where $\theta = 0$ is discussed in Appendix A.

Proposition 1 (conservation): For an arbitrary function $f(t, \boldsymbol{X}, \boldsymbol{\xi}, \mathscr{E})$, the following relation holds:

$$\iint_0^\infty \varphi_r Q(f) d\mathscr{E} d\boldsymbol{\xi} = 0, \tag{16}$$

where φ_r ($r = 0, ..., 4$) are the collision invariants, i.e.,

$$\varphi_0 = 1, \qquad \varphi_i = \xi_i \quad (i = 1, 2, 3), \qquad \varphi_4 = \frac{1}{2}|\boldsymbol{\xi}|^2 + \mathscr{E}. \tag{17}$$

Proposition 2 (equilibrium): The vanishing of the collision term $Q(f) = 0$ is equivalent to the fact that f is the following local equilibrium distribution:

$$f_{\mathrm{eq}} = \frac{\bar{\rho}\mathscr{E}^{\bar{\delta}/2-1}}{(2\pi R\bar{T})^{3/2}(R\bar{T})^{\bar{\delta}/2}\Gamma(\bar{\delta}/2)} \exp\left(-\frac{|\boldsymbol{\xi} - \bar{\boldsymbol{v}}|^2}{2R\bar{T}} - \frac{\mathscr{E}}{R\bar{T}}\right), \tag{18}$$

where $\bar{\rho}$, $\bar{\boldsymbol{v}}$, and $\bar{T}$ are arbitrary functions of t and $\boldsymbol{X}$, and $\bar{\delta} = D(\bar{T})$.

Proposition 3: For an arbitrary function $f(t, \boldsymbol{X}, \boldsymbol{\xi}, \mathscr{E})$, the following inequality holds:

$$\iint_0^\infty \left(\ln \frac{f}{\mathscr{E}^{\delta/2-1}}\right) Q(f) d\mathscr{E} d\boldsymbol{\xi} \le 0, \tag{19}$$

and the equality sign holds if and only if $f = f_{\mathrm{eq}}$ in (18).

Now, we give the outlines of the proofs for Propositions 1, 2, and 3.

Proof of Proposition 1: From the definition, it follows immediately that

$$\iint_0^\infty f d\mathscr{E} d\boldsymbol{\xi} = \rho, \qquad \iint_0^\infty \xi_i f d\mathscr{E} d\boldsymbol{\xi} = \rho v_i, \qquad \iint_0^\infty \mathscr{E} f d\mathscr{E} d\boldsymbol{\xi} = \rho e_{\mathrm{int}}, \tag{20a}$$

$$\iint_0^\infty \xi_i \xi_j f d\mathscr{E} d\boldsymbol{\xi} = p_{ij} + \rho v_i v_j, \qquad \iint_0^\infty \xi_k^2 f d\mathscr{E} d\boldsymbol{\xi} = 2\rho e_{\mathrm{tr}} + \rho v_k^2, \tag{20b}$$

$$\iint_0^\infty \left(\frac{1}{2}\xi_k^2 + \mathscr{E}\right) f d\mathscr{E} d\boldsymbol{\xi} = \rho e + \frac{1}{2}\rho v_k^2. \tag{20c}$$

On the other hand, the moments of $\mathscr{G}$ are obtained, in the same way as Appendix A1 in [27], in the following form:

$$\iint_0^\infty \mathscr{G} d\mathscr{E} d\boldsymbol{\xi} = \rho, \quad \iint_0^\infty \xi_i \mathscr{G} d\mathscr{E} d\boldsymbol{\xi} = \rho v_i, \quad \iint_0^\infty \mathscr{E}\mathscr{G} d\mathscr{E} d\boldsymbol{\xi} = \rho \frac{\delta R T_{\mathrm{rel}}}{2}, \tag{21a}$$

$$\iint_0^\infty \xi_i \xi_j \mathscr{G} d\mathscr{E} d\boldsymbol{\xi} = \rho(\mathsf{T})_{ij} + \rho v_i v_j,$$

$$\iint_0^\infty \xi_k^2 \mathscr{G} d\mathscr{E} d\boldsymbol{\xi} = 3(1-\theta)R\rho T_{\mathrm{tr}} + 3\theta R\rho T + \rho v_k^2, \tag{21b}$$

$$\iint_0^\infty \left(\frac{1}{2}\xi_k^2 + \mathscr{E}\right) \mathscr{G} d\mathscr{E} d\boldsymbol{\xi} = \frac{3+\delta}{2} R\rho T + \frac{1}{2}\rho v_k^2 = \rho e + \frac{1}{2}\rho v_k^2, \tag{21c}$$

where $\delta = D(T)$ and $e = E(T)$, together with (4), have been used to obtain the last equality in (21c). Equation (16) with (17) follows directly from (20) and (21). $\square$

Proof of Proposition 2: We first suppose that $f = f_{\mathrm{eq}}$ and show that $\mathscr{G}$ reduces to f_{eq}, i.e., $Q(f) = 0$. It follows from (8c), (8d), and (9) that $\rho = \bar{\rho}$, $\boldsymbol{v} = \bar{\boldsymbol{v}}$, $p_{ij} = \bar{\rho} R\bar{T}\delta_{ij}$, $e_{\mathrm{tr}} = 3R\bar{T}/2$, $e_{\mathrm{int}} = \bar{\delta} R\bar{T}/2$, and $e = (3+\bar{\delta})R\bar{T}/2$. Because of $\bar{\delta} = D(\bar{T})$ and (4), we find that $e = [3+D(\bar{T})]R\bar{T}/2 = E(\bar{T})$. Therefore, from (8e), we obtain $T = \bar{T}$ and $\delta = \bar{\delta}$. Then, (8f) gives $T_{\mathrm{tr}} = T_{\mathrm{int}} = T_{\mathrm{rel}} = \bar{T}$, so that (8b) leads to $(\mathsf{T})_{ij} = R\bar{T}\delta_{ij}$. Since $\det(\mathsf{T}) = (R\bar{T})^3$ and $(\mathsf{T}^{-1})_{ij} = \delta_{ij}/R\bar{T}$, we obtain $\mathscr{G} = f_{\mathrm{eq}}$. Therefore, $Q(f) = 0$ holds.

Conversely, we show that if we suppose $Q(f) = 0$, then f is of the form of (18) with appropriate $\bar{\rho}$, $\bar{\boldsymbol{v}}$, $\bar{T}$, and $\bar{\delta} = D(\bar{T})$ and does not take other functional forms. Suppose that $f = \mathscr{G}$ holds, where $\mathscr{G}$ is constructed on the basis of f. Then, by replacing f with $\mathscr{G}$ in (8c), (8d), and (9) and referring to (21), we obtain $\rho = \rho$, $\boldsymbol{v} = \boldsymbol{v}$, $p_{ij} = \rho(\mathsf{T})_{ij}$, $e_{\mathrm{tr}} = p_{kk}/2\rho = (\mathsf{T})_{kk}/2$, $e_{\mathrm{int}} = \delta R T_{\mathrm{rel}}/2$. With these results, (8b) and (8f) give the following relations:

$$[1-(1-\theta)\nu](\mathsf{T})_{ij} = (1-\theta)(1-\nu)RT_{\mathrm{tr}}\delta_{ij} + \theta RT\delta_{ij}, \tag{22a}$$

$$T_{\mathrm{tr}} = (\mathsf{T})_{kk}/3R, \qquad T_{\mathrm{int}} = T_{\mathrm{rel}}. \tag{22b}$$

Substituting $(\mathsf{T})_{kk}$ obtained from (22a) into the first equation of (22b), we obtain $\theta(T - T_{\mathrm{tr}}) = 0$. Using the second equation of (22b) in the last equation of (8f), we have $\theta(T - T_{\mathrm{int}}) = 0$. Because $\theta \neq 0$, $T_{\mathrm{tr}} = T_{\mathrm{int}} = T$ holds. In this case, (22a) gives $(\mathsf{T})_{ij} = RT\delta_{ij}$, so that $(\mathsf{T})_{kk} = 3RT$ and thus $e = e_{\mathrm{tr}} + e_{\mathrm{int}} = (3+\delta)RT/2$ hold. Noting that $e = E(T)$ and $\delta = D(T)$, we recover (4). Since $\det(\mathsf{T}) = (RT)^3$ and $(\mathsf{T}^{-1})_{ij} = \delta_{ij}/RT$, $\mathscr{G}$ and thus f are reduced to f_{eq} with $\bar{\rho} = \rho$, $\bar{\boldsymbol{v}} = \boldsymbol{v}$, $\bar{T} = T$, and $\bar{\delta} = \delta = D(T)$. $\square$

Proof of Proposition 3: For each t and X, the quantity δ, which is a function of T, is a constant. Therefore, the proof for the model equation with constant δ, which is given in [2], holds for the present model. $\square$

Here, we should note that Proposition 3 does not lead to the H theorem. Let us define $H_\delta(f)$ by

$$H_\delta(f) = \iint_0^\infty f \ln \frac{f}{\mathscr{E}^{\delta/2-1}} d\mathscr{E} d\boldsymbol{\xi}. \tag{23}$$

If we multiply (6) by $1 + \ln(f/\mathscr{E}^{\delta/2-1})$ and integrate with respect to $\mathscr{E}$ from 0 to ∞ and with respect to $\boldsymbol{\xi}$ over the whole space, we can show that the right-hand side is nonnegative because of Proposition 3. However, the left-hand side cannot be reduced to the form of the H theorem because δ depends on t and $\boldsymbol{X}$ through T. We can only show the following:

Proposition 4 (*H* theorem for spatially homogeneous case): If f does not depend on $\boldsymbol{X}$, the following inequality holds:

$$dH_\delta/dt \leq 0, \tag{24}$$

and the equality sign holds if and only if f is the local equilibrium f_{eq} [cf. (18)].

Proof of Proposition 4: If $f = f(t, \boldsymbol{\xi})$, (6) reduces to $\partial f/\partial t = Q(f)$. We multiply this equation by $(1/2)|\boldsymbol{\xi} - \boldsymbol{v}|^2 + \mathscr{E}$, integrate with respect to $\mathscr{E}$ from 0 to ∞ and with respect to $\boldsymbol{\xi}$ over the whole space, and make use of (9) and (16). Then, we have $de/dt = 0$. This means that T is constant, so that δ is constant. Therefore, if we differentiate (23) with respect to t, we have

$$\frac{dH_\delta}{dt} = \iint_0^\infty \left(1 + \ln \frac{f}{\mathscr{E}^{\delta/2-1}}\right) \frac{\partial f}{\partial t} d\mathscr{E} d\boldsymbol{\xi} = \iint_0^\infty \left(\ln \frac{f}{\mathscr{E}^{\delta/2-1}}\right) Q(f) d\mathscr{E} d\boldsymbol{\xi} \leq 0, \tag{25}$$

because of Proposition 3. □

2.3 Transport coefficients

With the model proposed in Sect. 2.1, we can carry out the Chapman–Enskog expansion [18, 22, 48] to obtain the Navier–Stokes equations for a compressible fluid (the so-called compressible Navier–Stokes equations) and the associated transport coefficients. In this section, we just summarize the results of the Navier–Stokes equations and the transport coefficients omitting the process, since the Chapman–Enskog expansion is a standard procedure. The details of the analysis will be given elsewhere. In this section, we assume that $\theta \neq 0$.

The compressible Navier–Stokes equations derived by the Chapman–Enskog expansion are summarized as follows:

$$\frac{\partial \rho}{\partial t} + \frac{\partial \rho v_j}{\partial X_j} = 0, \tag{26a}$$

$$\begin{aligned}\frac{\partial \rho v_i}{\partial t} + \frac{\partial \rho v_i v_j}{\partial X_j} = -\frac{\partial p}{\partial X_i} + \frac{\partial}{\partial X_j}\left[\mu(T)\left(\frac{\partial v_i}{\partial X_j} + \frac{\partial v_j}{\partial X_i} - \frac{2}{3}\frac{\partial v_k}{\partial X_k}\delta_{ij}\right)\right] \\ + \frac{\partial}{\partial X_i}\left[\mu_b(T)\frac{\partial v_k}{\partial X_k}\right],\end{aligned} \tag{26b}$$

$$\begin{aligned}\frac{\partial}{\partial t}\left[\rho\left(\frac{3+D(T)}{2}RT + \frac{1}{2}|\boldsymbol{v}|^2\right)\right] + \frac{\partial}{\partial X_j}\left[\rho v_j\left(\frac{5+D(T)}{2}RT + \frac{1}{2}|\boldsymbol{v}|^2\right)\right] \\ = \frac{\partial}{\partial X_j}\left[\lambda(T)\frac{\partial T}{\partial X_j}\right] + \frac{\partial}{\partial X_j}\left[\mu(T) v_i\left(\frac{\partial v_i}{\partial X_j} + \frac{\partial v_j}{\partial X_i} - \frac{2}{3}\frac{\partial v_k}{\partial X_k}\delta_{ij}\right)\right] \\ + \frac{\partial}{\partial X_j}\left[\mu_b(T) v_j \frac{\partial v_k}{\partial X_k}\right],\end{aligned} \tag{26c}$$

with $p = R\rho T$ [cf. (12a)]. Here, the viscosity $\mu(T)$, the bulk viscosity $\mu_b(T)$, and the thermal conductivity $\lambda(T)$ are, respectively, given by

$$\mu(T) = \frac{1}{1-\nu+\theta\nu}\frac{RT}{A_c(T)}, \tag{27a}$$

$$\mu_b(T) = \frac{1}{\theta}\left[\frac{2}{3} - \frac{R}{C_v(T)}\right]\frac{RT}{A_c(T)}, \tag{27b}$$

$$\lambda(T) = [C_v(T) + R]\frac{RT}{A_c(T)}. \tag{27c}$$

Let us denote by Pr the Prandtl number defined by $\mathrm{Pr} = C_p\mu/\lambda = (C_v + R)\mu/\lambda$. Then, we have the following expression of Pr:

$$\mathrm{Pr} = \frac{1}{1-\nu+\theta\nu}. \tag{28}$$

Making use of (28) and the ratio of the specific heats γ [cf. (5)], we can rewrite μ_b and λ in the following form:

$$\mu_b(T) = \frac{1}{\theta}\left[\frac{5}{3} - \gamma(T)\right]\frac{\mu(T)}{\mathrm{Pr}}, \qquad \lambda(T) = \frac{\gamma(T)R}{\gamma(T)-1}\frac{RT}{A_c(T)}. \tag{29}$$

3 Shock-wave structure

In this section, we apply the model equation proposed in Sect. 2 to the problem of shock-wave structure. The shock wave is a compression wave across which the physical quantities undergo rapid changes over a distance of some tens of the mean free path. Therefore, to describe the structure inside the shock wave, one has to use kinetic theory or the Boltzmann equation. In fact, the structure of a standing plane shock wave is one of the most fundamental problems in kinetic theory and has been investigated by many authors. Since the survey of previous work is beyond the scope of the present paper, we just refer to some standard textbooks [26,20,15, 8,16,48] containing this subject and move on to the problem that will be tackled in the present paper, that is, the shock-wave structure for a polyatomic gas with large bulk viscosity.

Motivated by some recent and interesting results based on extended thermodynamics [51,52,45,53], we investigated the structure of a plane shock wave in carbon dioxide (CO_2) gas, which is known to have very large bulk viscosity, numerically using the ES model for a gas with constant specific heats (calorically perfect or polytropic gas) [28,27]. In [27], some comparisons were made between the result based on the ES model and that based on extended thermodynamics [52], and good agreement was shown. However, the comparisons were restricted to rather weak shock waves in which the temperature variation is not large. The reason is that [52,53] used the data for CO_2 gas with temperature-dependent specific heats, whereas [27] used the ES model with constant specific heats. For a strong shock wave, the effect of temperature-dependent specific heats becomes more important because of the large temperature variation across the shock. In order to understand this effect, we try to carry out the numerical analysis of the shock profile, with special interest in stronger shock waves, using the model for a gas with temperature-dependent specific heats (thermally perfect or non-polytropic gas) proposed in Sect. 2.

3.1 Problem

Let us consider a stationary plane shock wave standing in a flow of an ideal polyatomic gas. We take the X_1 axis perpendicular to the shock wave. The gas at upstream infinity ($X_1 \to -\infty$) is in an equilibrium state with density ρ_-, flow velocity $\boldsymbol{v}_- = (v_-, 0, 0)$ ($v_- > 0$), and temperature T_-, and that at downstream infinity ($X_1 \to \infty$) is in another equilibrium state with density ρ_+, flow velocity $\boldsymbol{v}_+ = (v_+, 0, 0)$ ($v_+ > 0$), and temperature T_+. We investigate the steady behavior of the gas under the following assumptions:

(i) The specific heat at constant volume C_v is a given function $C_v(T)$ of the temperature T (thermally perfect or non-polytropic gas).
(ii) The behavior of the gas is described by the ES model of the Boltzmann equation proposed in Sect. 2.
(iii) The problem is spatially one dimensional, so that the physical quantities are independent of X_2 and X_3.

Let us denote by M_- the Mach number of the flow at upstream infinity and by γ_- the ratio of the specific heats there, i.e.,

$$M_- = \frac{v_-}{\sqrt{\gamma_- R T_-}}, \qquad \gamma_- = \gamma(T_-) = \frac{C_v(T_-) + R}{C_v(T_-)}. \tag{30}$$

The downstream quantities ρ_+, v_+, and T_+ are related with the upstream quantities ρ_-, v_-, and T_- and the upstream Mach number M_- by the Rankine–Hugoniot relations. To be more specific,

Proposition 5 (Rankine–Hugoniot relations): When $\theta \neq 0$, the ratios ρ_+/ρ_-, v_+/v_-, and T_+/T_- are expressed in the following form:

$$\frac{\rho_+}{\rho_-} = \left(\frac{v_+}{v_-}\right)^{-1}, \qquad \frac{v_+}{v_-} = \frac{1 + \gamma_- M_-^2 - \sqrt{2\gamma_- M_-^2 \hat{d}_E(\tau) + 1}}{\gamma_- M_-^2}, \qquad \frac{T_+}{T_-} = \tau, \tag{31}$$

where the function $\hat{d}_E(x)$ is defined by

$$\hat{d}_E(x) = \frac{1}{R}\int_1^x C_v(T_- s)\,ds, \tag{32}$$

and τ is the solution, such that $\tau > 1$, of the following equation:

$$\tau + 2\hat{d}_E(\tau) + \frac{1}{\gamma_- M_-^2} - \left(\frac{1}{\sqrt{\gamma_-}M_-} + \sqrt{\gamma_-}M_-\right)\sqrt{2\hat{d}_E(\tau) + \frac{1}{\gamma_- M_-^2}} = 0. \tag{33}$$

If $C_v(T)$ is a monotonically increasing function of T, such τ is unique.

The proof of Proposition 5 is given in Appendix B.1. Although we have not been able to show that the Mach number at downstream infinity, $M_+ = v_+/(\gamma_+ RT_+)^{1/2}$ where $\gamma_+ = \gamma(T_+)$, is less than 1 for M_- greater than 1, we have confirmed it numerically. Therefore, we will assume that $M_- > 1$ and $M_+ < 1$ throughout the present paper. The Rankine–Hugoniot relations take a different form when $\theta = 0$. They are shown as Proposition 5′ in Appendix B.2. For a gas with large bulk viscosity such as CO_2 gas, the shock profiles exhibit a double layer structure consisting of a thin front layer and a thick rear layer, except for M_- relatively close to 1. It is shown in [27] that the thin front shock is nothing but a shock wave for $\theta = 0$ ($\mu_b/\mu = \infty$) whose jumps are described by the Rankine–Hugoniot relations given as Proposition 5′.

3.2 Basic equation

The present shock-structure problem is a time-independent and spatially one-dimensional problem where f is expressed as $f = f(X_1, \boldsymbol{\xi}, \mathscr{E})$. Therefore, the basic equation is (6) with $\partial f/\partial t = \partial f/\partial X_2 = \partial f/\partial X_3 = 0$. Consistently, all the macroscopic quantities in (7)–(9) and (12) are the functions of X_1 only, and $\boldsymbol{v} = (v_1, 0, 0)$.

The boundary conditions at upstream and downstream infinities are expressed in the following form using the equilibrium distribution (18):

$$f = \frac{\rho_- \mathscr{E}^{\delta_-/2-1}}{(2\pi RT_-)^{3/2}(RT_-)^{\delta_-/2}\Gamma(\delta_-/2)} \exp\left(-\frac{(\xi_1 - v_-)^2 + \xi_2^2 + \xi_3^2}{2RT_-} - \frac{\mathscr{E}}{RT_-}\right), \quad (X_1 \to -\infty), \tag{34a}$$

$$f = \frac{\rho_+ \mathscr{E}^{\delta_+/2-1}}{(2\pi RT_+)^{3/2}(RT_+)^{\delta_+/2}\Gamma(\delta_+/2)} \exp\left(-\frac{(\xi_1 - v_+)^2 + \xi_2^2 + \xi_3^2}{2RT_+} - \frac{\mathscr{E}}{RT_+}\right), \quad (X_1 \to \infty), \tag{34b}$$

where we have let $\delta_- = D(T_-)$ and $\delta_+ = D(T_+)$.

Now, we introduce the dimensionless quantities (x_1, ζ_i, $\hat{\mathscr{E}}$, $\hat{f}$, $\hat{\mathscr{G}}$, $\hat{A}_c$, $\hat{\rho}$, $\hat{v}_i$, $\hat{p}_{ij}$, $\hat{e}_{\rm tr}$, $\hat{e}_{\rm int}$, $\hat{e}$, $\hat{T}_{\rm tr}$, $\hat{T}_{\rm int}$, $\hat{T}$, $\hat{T}_{\rm rel}$, $\hat{\mathsf{T}}_{ij}$, $\hat{p}$, $\hat{q}_i$, $\hat{E}$, $\hat{C}_v$) corresponding to (X_1, ξ_i, $\mathscr{E}$, f, $\mathscr{G}$, A_c, ρ, v_i, p_{ij}, $e_{\rm tr}$, $e_{\rm int}$, e, $T_{\rm tr}$, $T_{\rm int}$, T, $T_{\rm rel}$, T_{ij}, p, q_i, E, C_v) by the following relations:

$$x_1 = X_1/l_-, \qquad \zeta_i = \xi_i/(2RT_-)^{1/2}, \qquad \hat{\mathscr{E}} = \mathscr{E}/RT_-, \tag{35a}$$

$$(\hat{f}, \hat{\mathscr{G}}) = (f, \mathscr{G})(2RT_-)^{5/2}/2\rho_-, \qquad \hat{A}_c(\hat{T}) = A_c(T)/A_c(T_-), \tag{35b}$$

$$\hat{\rho} = \rho/\rho_-, \qquad \hat{v}_i = v_i/(2RT_-)^{1/2}, \qquad \hat{p}_{ij} = p_{ij}/p_-, \tag{35c}$$

$$(\hat{e}_{\rm tr}, \hat{e}_{\rm int}, \hat{e}) = (e_{\rm tr}, e_{\rm int}, e)/RT_-, \qquad (\hat{T}_{\rm tr}, \hat{T}_{\rm int}, \hat{T}, \hat{T}_{\rm rel}) = (T_{\rm tr}, T_{\rm int}, T, T_{\rm rel})/T_-, \tag{35d}$$

$$\hat{\mathsf{T}}_{ij} = \mathsf{T}_{ij}/RT_-, \qquad \hat{p} = p/p_-, \qquad \hat{q}_i = q_i/p_-(2RT_-)^{1/2}, \tag{35e}$$

$$\hat{E}(\hat{T}) = E(T)/RT_-, \qquad \hat{C}_v(\hat{T}) = C_v(T)/R, \tag{35f}$$

where $p_- = R\rho_- T_-$, and $l_- = (2/\sqrt{\pi})(2RT_-)^{1/2}/A_c(T_-)\rho_-$ is the mean free path of the gas molecules in the equilibrium state at rest at density ρ_- and temperature T_-.

By using these dimensionless variables, (6) (with $\partial f/\partial t = \partial f/\partial X_2 = \partial f/\partial X_3 = 0$) and (7)–(9) are recast in the following dimensionless form:

$$\zeta_1 \frac{\partial \hat{f}}{\partial x_1} = \frac{2}{\sqrt{\pi}} \hat{Q}(\hat{f}), \tag{36}$$

with

$$\hat{Q}(\hat{f}) = \hat{A}_c(\hat{T})\hat{\rho}\left(\hat{\mathscr{G}} - \hat{f}\right). \tag{37}$$

Here,

$$\hat{\mathscr{G}} = \frac{\hat{\rho}\hat{\mathscr{E}}^{\delta/2-1}}{\pi^{3/2}[\det(\hat{\mathsf{T}})]^{1/2}\, \hat{T}_{\mathrm{rel}}^{\delta/2}\Gamma(\delta/2)} \times \exp\left(-(\hat{\mathsf{T}}^{-1})_{ij}(\zeta_i - \hat{v}_i)(\zeta_j - \hat{v}_j) - \frac{\hat{\mathscr{E}}}{\hat{T}_{\mathrm{rel}}}\right), \tag{38a}$$

$$(\hat{\mathsf{T}})_{ij} = (1-\theta)[(1-\nu)\hat{T}_{\mathrm{tr}}\delta_{ij} + \nu \hat{p}_{ij}/\hat{\rho}] + \theta \hat{T}\delta_{ij}, \tag{38b}$$

$$\hat{\rho} = \iint_0^\infty \hat{f}\, d\hat{\mathscr{E}}\, d\boldsymbol{\zeta}, \qquad \hat{v}_i = \frac{1}{\hat{\rho}}\iint_0^\infty \zeta_i \hat{f}\, d\hat{\mathscr{E}}\, d\boldsymbol{\zeta}, \tag{38c}$$

$$\hat{p}_{ij} = 2\iint_0^\infty (\zeta_i - \hat{v}_i)(\zeta_j - \hat{v}_j)\hat{f}\, d\hat{\mathscr{E}}\, d\boldsymbol{\zeta}, \tag{38d}$$

$$\hat{T} = \hat{E}^{-1}(\hat{e}), \qquad \delta = \hat{D}(\hat{T}), \tag{38e}$$

$$\hat{T}_{\mathrm{tr}} = 2\hat{e}_{\mathrm{tr}}/3, \qquad \hat{T}_{\mathrm{int}} = 2\hat{e}_{\mathrm{int}}/\delta, \qquad \hat{T}_{\mathrm{rel}} = \theta\hat{T} + (1-\theta)\hat{T}_{\mathrm{int}}, \tag{38f}$$

where

$$\hat{e} = \hat{e}_{\mathrm{tr}} + \hat{e}_{\mathrm{int}}, \qquad \hat{e}_{\mathrm{tr}} = \frac{1}{\hat{\rho}}\iint_0^\infty |\boldsymbol{\zeta} - \hat{\boldsymbol{v}}|^2 \hat{f}\, d\hat{\mathscr{E}}\, d\boldsymbol{\zeta}, \qquad \hat{e}_{\mathrm{int}} = \frac{1}{\hat{\rho}}\iint_0^\infty \hat{\mathscr{E}}\hat{f}\, d\hat{\mathscr{E}}\, d\boldsymbol{\zeta}, \tag{39}$$

and $\hat{E}(\hat{T})$, whose inverse function is denoted by $\hat{E}^{-1}$, and $\hat{D}(\hat{T})$, which are the dimensionless versions of $E(T)$ [cf. (3)] and $D(T)$ [cf. (4)], respectively, are defined by

$$\hat{E}(\hat{T}) = \int_{\hat{T}_*}^{\hat{T}} \hat{C}_v(s)\, ds + \hat{E}_*, \tag{40a}$$

$$\hat{D}(\hat{T}) = \frac{2}{\hat{T}}\hat{E}(\hat{T}) - 3\ [= D(T)], \tag{40b}$$

with $\hat{T}_* = T_*/T_-$ and $\hat{E}_* = E_*/RT_-$. Then, we find that the following relations hold:

$$\hat{e} = \frac{3+\delta}{2}\hat{T}, \qquad \hat{T} = \frac{3\hat{T}_{\mathrm{tr}} + \delta\hat{T}_{\mathrm{int}}}{3+\delta}. \tag{41}$$

Incidentally, the dimensionless pressure and heat-flow vector are expressed as

$$\hat{p} = \hat{\rho}\hat{T}, \qquad \hat{q}_i = \iint_0^\infty (\zeta_i - \hat{v}_i)\left(|\boldsymbol{\zeta} - \hat{\boldsymbol{v}}|^2 + \hat{\mathscr{E}}\right)\hat{f}d\hat{\mathscr{E}}d\boldsymbol{\zeta}. \tag{42}$$

The dimensionless form of the boundary conditions (34) is given by the following equations:

$$\hat{f} = \frac{\hat{\mathscr{E}}^{\delta_-/2-1}}{\pi^{3/2}\Gamma(\delta_-/2)}\exp\left(-\left[(\zeta_1 - \hat{v}_-)^2 + \zeta_2^2 + \zeta_3^2\right] - \hat{\mathscr{E}}\right), \qquad (x_1 \to -\infty), \tag{43a}$$

$$\hat{f} = \frac{\hat{\rho}_+\hat{\mathscr{E}}^{\delta_+/2-1}}{(\pi\hat{T}_+)^{3/2}\hat{T}_+^{\delta_+/2}\Gamma(\delta_+/2)}\exp\left(-\frac{(\zeta_1 - \hat{v}_+)^2 + \zeta_2^2 + \zeta_3^2}{\hat{T}_+} - \frac{\hat{\mathscr{E}}}{\hat{T}_+}\right), \quad (x_1 \to \infty), \tag{43b}$$

where

$$\hat{v}_- = \frac{v_-}{(2RT_-)^{1/2}} = \sqrt{\frac{\gamma_-}{2}}M_-, \quad \hat{v}_+ = \frac{v_+}{(2RT_-)^{1/2}}, \quad \hat{\rho}_+ = \frac{\rho_+}{\rho_-}, \quad \hat{T}_+ = \frac{T_+}{T_-}, \tag{44}$$

and $\delta_- = \hat{D}(1)$ and $\delta_+ = \hat{D}(\hat{T}_+)$. Note that

$$(\hat{\rho}, \hat{v}, \hat{T}_{\mathrm{tr}}, \hat{T}_{\mathrm{int}}) \to \begin{cases} (1, \hat{v}_-, 1, 1), & \text{as } x_1 \to -\infty, \\ (\hat{\rho}_+, \hat{v}_+, \hat{T}_+, \hat{T}_+), & \text{as } x_1 \to \infty, \end{cases} \tag{45}$$

and $\hat{\rho}_+$, $\hat{v}_+$, and $\hat{T}_+$ are given by the dimensionless version of the Rankine–Hugoniot relations (31).

3.3 Similarity solution

We consider the similarity solution of the form

$$\hat{f} = \hat{f}(x_1, \zeta_1, \zeta_\rho, \hat{\mathscr{E}}), \qquad \zeta_\rho = (\zeta_2^2 + \zeta_3^2)^{1/2}, \tag{46}$$

which is compatible with the present problem. Then, the macroscopic quantities are expressed as

$$\hat{\rho} = 2\pi\int_0^\infty\int_{-\infty}^\infty\int_0^\infty \zeta_\rho \hat{f} d\hat{\mathscr{E}} d\zeta_1 d\zeta_\rho, \tag{47a}$$

$$\hat{v}_1 = \frac{2\pi}{\hat{\rho}}\int_0^\infty\int_{-\infty}^\infty\int_0^\infty \zeta_\rho\zeta_1 \hat{f} d\hat{\mathscr{E}} d\zeta_1 d\zeta_\rho, \tag{47b}$$

$$\hat{v}_2 = \hat{v}_3 = 0, \tag{47c}$$

$$\hat{p}_{11} = 4\pi\int_0^\infty\int_{-\infty}^\infty\int_0^\infty \zeta_\rho(\zeta_1 - \hat{v}_1)^2 \hat{f} d\hat{\mathscr{E}} d\zeta_1 d\zeta_\rho, \tag{47d}$$

$$\hat{p}_{22} = \hat{p}_{33} = 2\pi\int_0^\infty\int_{-\infty}^\infty\int_0^\infty \zeta_\rho^3 \hat{f} d\hat{\mathscr{E}} d\zeta_1 d\zeta_\rho, \tag{47e}$$

$$\hat{p}_{12} = \hat{p}_{13} = \hat{p}_{23} = 0, \tag{47f}$$

$$\hat{e}_{\mathrm{tr}} = \frac{2\pi}{\hat{\rho}} \int_0^\infty \int_{-\infty}^\infty \int_0^\infty \zeta_\rho \left[(\zeta_1 - \hat{v}_1)^2 + \zeta_\rho^2 \right] \hat{f} d\hat{\mathscr{E}} d\zeta_1 d\zeta_\rho, \tag{47g}$$

$$\hat{e}_{\mathrm{int}} = \frac{2\pi}{\hat{\rho}} \int_0^\infty \int_{-\infty}^\infty \int_0^\infty \zeta_\rho \hat{\mathscr{E}} \hat{f} d\hat{\mathscr{E}} d\zeta_1 d\zeta_\rho, \tag{47h}$$

$$\hat{q}_1 = 2\pi \int_0^\infty \int_{-\infty}^\infty \int_0^\infty \zeta_\rho (\zeta_1 - \hat{v}_1) \left[(\zeta_1 - \hat{v}_1)^2 + \zeta_\rho^2 + \hat{\mathscr{E}} \right] \hat{f} d\hat{\mathscr{E}} d\zeta_1 d\zeta_\rho, \tag{47i}$$

$$\hat{q}_2 = \hat{q}_3 = 0. \tag{47j}$$

In addition, $\hat{\mathscr{G}}$ is reduced to the following form:

$$\hat{\mathscr{G}} = \frac{\hat{\rho} \hat{\mathscr{E}}^{\delta/2-1}}{\pi^{3/2} [(\hat{\mathsf{T}})_{11}]^{1/2} (\hat{\mathsf{T}})_{22} \, \hat{T}_{\mathrm{rel}}^{\delta/2} \Gamma(\delta/2)} \exp\left(-\frac{(\zeta_1 - \hat{v}_1)^2}{(\hat{\mathsf{T}})_{11}} - \frac{\zeta_\rho^2}{(\hat{\mathsf{T}})_{22}} - \frac{\hat{\mathscr{E}}}{\hat{T}_{\mathrm{rel}}} \right), \tag{48}$$

where

$$(\hat{\mathsf{T}})_{11} = (1-\theta)[(1-\nu)\hat{T}_{\mathrm{tr}} + \nu \hat{p}_{11}/\hat{\rho}] + \theta \hat{T}, \tag{49a}$$

$$(\hat{\mathsf{T}})_{22} = (\hat{\mathsf{T}})_{33} = (1-\theta)[(1-\nu)\hat{T}_{\mathrm{tr}} + \nu \hat{p}_{22}/\hat{\rho}] + \theta \hat{T}, \tag{49b}$$

$$(\hat{\mathsf{T}})_{12} = (\hat{\mathsf{T}})_{13} = (\hat{\mathsf{T}})_{23} = 0. \tag{49c}$$

3.4 Further reduction

Let us introduce the following three marginal distribution functions ϕ_1, ϕ_2, and ϕ_3:

$$\phi_1(x_1, \zeta_1) = 2\pi \int_0^\infty \int_0^\infty \zeta_\rho \hat{f}(x_1, \zeta_1, \zeta_\rho, \hat{\mathscr{E}}) d\hat{\mathscr{E}} d\zeta_\rho, \tag{50a}$$

$$\phi_2(x_1, \zeta_1) = 2\pi \int_0^\infty \int_0^\infty \zeta_\rho^3 \hat{f}(x_1, \zeta_1, \zeta_\rho, \hat{\mathscr{E}}) d\hat{\mathscr{E}} d\zeta_\rho, \tag{50b}$$

$$\phi_3(x_1, \zeta_1) = 2\pi \int_0^\infty \int_0^\infty \zeta_\rho \hat{\mathscr{E}} \hat{f}(x_1, \zeta_1, \zeta_\rho, \hat{\mathscr{E}}) d\hat{\mathscr{E}} d\zeta_\rho, \tag{50c}$$

whose independent variables are x_1 and ζ_1 only.

Now we use the similarity solution (46) and the resulting relations (47), (48), and (49) in (36). If we multiply this equation by $\zeta_\rho(1,\, \zeta_\rho^2,\, \hat{\mathscr{E}})$ and integrate the result with respect to $\hat{\mathscr{E}}$ and ζ_ρ from 0 to ∞ for the respective variables, we obtain the system of integro-differential equations for ϕ_1, ϕ_2, and ϕ_3, that is,

$$\zeta_1 \frac{\partial \phi_k}{\partial x_1} = \frac{2}{\sqrt{\pi}} \hat{A}_c(\hat{T}) \hat{\rho} \left(\Psi_k - \phi_k \right), \qquad (k = 1, 2, 3), \tag{51}$$

where

$$\begin{bmatrix} \Psi_1 \\ \Psi_2 \\ \Psi_3 \end{bmatrix} = \frac{\hat{\rho}}{[\pi (\hat{\mathsf{T}})_{11}]^{1/2}} \begin{bmatrix} 1 \\ (\hat{\mathsf{T}})_{22} \\ \hat{T}_{\mathrm{rel}} \delta/2 \end{bmatrix} \exp\left(-\frac{(\zeta_1 - \hat{v}_1)^2}{(\hat{\mathsf{T}})_{11}} \right), \tag{52a}$$

$$(\hat{\mathsf{T}})_{11} = (1-\theta)[(1-\nu)\hat{T}_{\mathrm{tr}} + \nu \hat{p}_{11}/\hat{\rho}] + \theta \hat{T}, \tag{52b}$$

$$(\hat{\mathsf{T}})_{22} = (1-\theta)[(1-\nu)\hat{T}_{\mathrm{tr}} + \nu\hat{p}_{22}/\hat{\rho}] + \theta\hat{T}, \tag{52c}$$

$$\hat{\rho} = \int_{-\infty}^{\infty}\phi_1 d\zeta_1, \qquad \hat{v}_1 = \frac{1}{\hat{\rho}}\int_{-\infty}^{\infty}\zeta_1\phi_1 d\zeta_1, \tag{52d}$$

$$\hat{p}_{11} = 2\int_{-\infty}^{\infty}(\zeta_1-\hat{v}_1)^2\phi_1 d\zeta_1, \qquad \hat{p}_{22} = \int_{-\infty}^{\infty}\phi_2 d\zeta_1, \tag{52e}$$

$$\hat{e}_{\mathrm{tr}} = \frac{1}{\hat{\rho}}\int_{-\infty}^{\infty}\left[(\zeta_1-\hat{v}_1)^2\phi_1+\phi_2\right]d\zeta_1, \qquad \hat{e}_{\mathrm{int}} = \frac{1}{\hat{\rho}}\int_{-\infty}^{\infty}\phi_3 d\zeta_1, \tag{52f}$$

$$\hat{e} = \hat{e}_{\mathrm{tr}} + \hat{e}_{\mathrm{int}}, \qquad \hat{T} = \hat{E}^{-1}(\hat{e}), \qquad \delta = \hat{D}(\hat{T}), \tag{52g}$$

$$\hat{T}_{\mathrm{tr}} = 2\hat{e}_{\mathrm{tr}}/3, \qquad \hat{T}_{\mathrm{int}} = 2\hat{e}_{\mathrm{int}}/\delta, \qquad \hat{T}_{\mathrm{rel}} = \theta\hat{T} + (1-\theta)\hat{T}_{\mathrm{int}}. \tag{52h}$$

In addition, the heat-flow vector is expressed as

$$\hat{q}_1 = \int_{-\infty}^{\infty}(\zeta_1-\hat{v}_1)\left[(\zeta_1-\hat{v}_1)^2\phi_1+\phi_2+\phi_3\right]d\zeta_1. \tag{53}$$

The boundary conditions for (51) can be obtained from (43) by the same procedure, i.e.,

$$\begin{bmatrix}\phi_1\\ \phi_2\\ \phi_3\end{bmatrix} = \frac{1}{\pi^{1/2}}\begin{bmatrix}1\\ 1\\ \delta_-/2\end{bmatrix}\exp\left(-(\zeta_1-\hat{v}_-)^2\right), \qquad (x_1 \to -\infty), \tag{54a}$$

$$\begin{bmatrix}\phi_1\\ \phi_2\\ \phi_3\end{bmatrix} = \frac{\hat{\rho}_+}{(\pi\hat{T}_+)^{1/2}}\begin{bmatrix}1\\ \hat{T}_+\\ \hat{T}_+\delta_+/2\end{bmatrix}\exp\left(-\frac{(\zeta_1-\hat{v}_+)^2}{\hat{T}_+}\right), \qquad (x_1 \to \infty). \tag{54b}$$

3.5 Numerical analysis

We solve the boundary-value problem for ϕ_1, ϕ_2, and ϕ_3, i.e., (51), (52), and (54), numerically by a finite-difference method. Since the method is essentially the same as that was used and explained in [27], we omit the description of the method in the present paper. The only difference lies in the determination of the temperature $\hat{T}$ at each iteration step. Therefore, we explain the procedure to determine $\hat{T}$ when the (dimensionless) specific heat at constant volume $\hat{C}_v$ is given as a polynomial of $\hat{T}$.

Let us assume that $\hat{C}_v$ is given by

$$\hat{C}_v(\hat{T}) = \sum_{k=0}^{N} c_k\hat{T}^k. \tag{55}$$

In the present problem, the minimum temperature T_* in (3) should be T_-, so that $E_* = E(T_-)$. Therefore, it follows from (4) that $E_* = E(T_-) = [3+D(T_-)]RT_-/2 = (3+\delta_-)RT_-/2$, or equivalently, $\hat{E}_*$ in (40a) is given as $\hat{E}_* = \hat{E}(1) = (3+\delta_-)/2$. Thus, from (40a), we have

$$\hat{E}(\hat{T}) = \int_1^{\hat{T}}\hat{C}_v(s)ds + \hat{E}(1) = \sum_{k=0}^{N}\frac{c_k}{k+1}(\hat{T}^{k+1}-1) + \frac{3+\delta_-}{2}. \tag{56}$$

Table 1 Downstream states for $M_- = 1.3$ and 5. The corresponding values for constant C_v $[C_v(T) = C_v(T_-)]$ are shown in the parentheses

	$M_- = 1.3$	$M_- = 5$
ρ_+/ρ_-	1.566 (1.554)	7.819 (6.199)
$v_+/(2RT_-)^{1/2}$	0.666 (0.671)	0.513 (0.648)
T_+/T_-	1.141 (1.143)	3.723 (4.522)
δ_+	3.940	5.910
$C_v(T_+)/R$	3.671	5.665
$\gamma(T_+)$	1.272	1.177

Table 2 Downstream states for $M_- = 1.3$ and 5 in the case of $\theta = 0$ (or $\mu_b/\mu = \infty$). See the caption of Table 1

	$M_- = 1.3$	$M_- = 5$
$\widetilde{M}_-$	1.143	4.398
ρ_+/ρ_-	1.214	3.463
$v_+/(2RT_-)^{1/2}$	0.860	1.159
T_+/T_-	1.060 (1.061)	2.947 (3.564)
$T_{\mathrm{tr}+}/T_-$	1.140	6.909
$T_{\mathrm{int}+}/T_-$	0.999	0.730
δ_+	3.918	5.362

Table 3 Values of ν and θ for $\mathrm{Pr} = 0.73$ and $(\mu_b/\mu)_{T=T_-} = 100$, 200, 500, 1000, 2000, 5200, and ∞

$(\mu_b/\mu)_{T=T_-}$	100	200	500	1000	2000	5200	∞
$-\nu \times 10$	3.718	3.708	3.702	3.701	3.700	3.699	3.699
$\theta \times 10^4$	51.69	25.85	10.34	5.169	2.585	0.9941	0

In order to obtain $\hat{T}$ satisfying $\hat{E}(\hat{T}) = \hat{e}$ for a given $\hat{e}$, we define the function $f(x)$ as

$$f(x) = \hat{E}(x) - \hat{e} = \sum_{k=0}^{N} \frac{c_k}{k+1}(x^{k+1} - 1) + \frac{3+\delta_-}{2} - \hat{e}, \tag{57}$$

and obtain the solution x of $f(x) = 0$ by the Newton method. That is, we construct the sequence $\{x_n\}$ by

$$x_{n+1} = x_n - \frac{f(x_n)}{f'(x_n)} = x_n - \frac{\hat{E}(x_n) - \hat{e}}{\hat{C}_v(x_n)} \qquad (n = 0, 1, 2, \ldots), \tag{58}$$

with an appropriate x_0 and obtain its limit as $n \to \infty$. Once $\hat{T}$ is obtained, δ is determined as $\delta = \hat{D}(\hat{T})$. This procedure is carried out at each step of iteration.

3.6 Numerical results

3.6.1 Parameter setting

We consider CO_2 gas and set the parameters basically following [52,53]. We set the upstream temperature T_- and pressure p_- to be $T_- = 295$ K and $p_- = 69$ mmHg, respectively, and use the formula $C_v(T)/R = 1.412 + 8.697 \times 10^{-3}T -$

$6.575 \times 10^{-6}T^2 + 1.987 \times 10^{-9}T^3$ for $C_v(T)$ derived in [53] from the experimental data, where the coefficients have suitable dimensions in such a way that each term on the right-hand side is dimensionless. Then we have $C_v(T_-)/R = 3.456$ and $\gamma_- = 1.289$. If we put $T_* = T_-$ and $E_* = T_- C_v(T_-)$ in (3) [cf. the last part of the paragraph containing (3)], we have $\delta_- = 2C_v(T_-)/R - 3 = 3.913$. In [52], it is assumed that $\mu \propto T^{0.935}$, so that we set $A_c(T) \propto T^{0.065}$ [or $\hat{A}_c(\hat{T}) = \hat{T}^{0.065}$] from (27a). It should be noted, however, that although $\mu_b \propto T^{0.935}$ and $\lambda \propto T^{0.935} C_v(T)/R$ are also assumed in [52], our model cannot be made to adjust to these forms because of (27b) and (27c). In other words, if the parameters ν and θ have been fixed, the choice of $C_v(T)$ and $A_c(T)$ completely determines μ, μ_b, and λ according to (27) in the present model. We determine the values of ν and θ from the values of Pr and μ_b/μ at $T = T_-$ using (28) and (29). More specifically, we set $\mathrm{Pr} = 0.73$ and consider some different values of μ_b/μ at $T = T_-$, i.e., $(\mu_b/\mu)_{T=T_-} = 100$, 200, 500, 1000, 2000, 5200, and ∞. The reason why we vary $(\mu_b/\mu)_{T=T_-}$ is that though μ_b/μ is known to be very large, the value is not known precisely and that we are interested in the behavior of a polyatomic gas when μ_b/μ becomes large. Therefore, as in [28] and [27], we consider a *pseudo*-CO_2 gas with variable $(\mu_b/\mu)_{T=T_-}$.

In [27], we showed the profiles of macroscopic quantities across a shock wave of Types A, B, and C, where these types are defined in [52]. That is, Type A indicates a smooth and symmetric profile that is realized when M_- is close to 1; Type C is a profile with a double-layer structure composed of a thin front layer with rapid change and a thick rear layer with slow relaxation of the internal modes that appears when M_- is slightly larger; and Type B indicates a non-symmetric profile with a corner upstream that occurs at the transition from Type A to Type C. The ES model with constant specific heats, which was used in [27], is legitimated for Type-A and B profiles because the temperature rise across the shock wave is small in these cases. Therefore, in the present study, we concentrate on the Type-C profile. Since the transition from Type A to Type C takes place at $M_- = 1.137$ in the present parameter setting, we carry out the computation for $M_- = 1.3$, 1.47, 3, and 5 following [52,53]. However, to save space, we will present the results only for $M_- = 1.3$ and 5. The downstream states for $M_- = 1.3$ and 5 are shown in Table 1, and the corresponding values for $\theta = 0$ (or $\mu_b/\mu = \infty$), including the values of $\widetilde{M}_-$ that is defined in Appendix B.2 [cf. (114b) with $T_{\mathrm{tr}-} = T_-$], are shown in Table 2. The values of ν and θ corresponding to our choices of Pr and $(\mu_b/\mu)_{T=T_-}$ are shown in Table 3.

3.6.2 *Profiles of macroscopic quantities*

As in [27], we show the profiles of the density ρ, the flow velocity v_1 (the X_1 component), and the temperatures T, T_{tr}, and T_{int} normalized in the conventional way, i.e.,

$$\check{\rho} = \frac{\rho - \rho_-}{\rho_+ - \rho_-}, \quad \check{v} = \frac{v_1 - v_+}{v_- - v_+}, \quad \check{T} = \frac{T - T_-}{T_+ - T_-}, \quad \check{T}_{\mathrm{tr}} = \frac{T_{\mathrm{tr}} - T_-}{T_+ - T_-}, \quad \check{T}_{\mathrm{int}} = \frac{T_{\mathrm{int}} - T_-}{T_+ - T_-}. \tag{59}$$

In this normalization, $\check{\rho}$, $\check{T}$, $\check{T}_{\mathrm{tr}}$, and $\check{T}_{\mathrm{int}}$ varies from 0 (upstream infinity) to 1 (downstream infinity), whereas $\check{v}$ from 1 (upstream infinity) to 0 (downstream in-

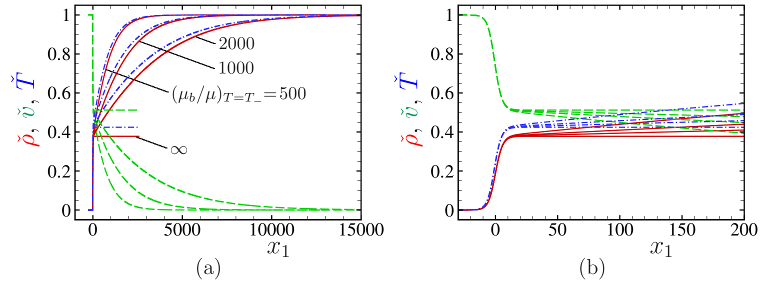

Fig. 1 Profiles of $\check{\rho}$, $\check{v}$, and $\check{T}$ at $M_- = 1.3$ for $(\mu_b/\mu)_{T=T_-} = 500$, 1000, 2000, and ∞. (a) Profiles for $-1000 \leq x_1 \leq 15000$, (b) profiles for $-30 \leq x_1 \leq 200$. The red solid line indicates $\check{\rho}$, the green dashed line $\check{v}$, and the blue dot-dashed line $\check{T}$. (Color figure online)

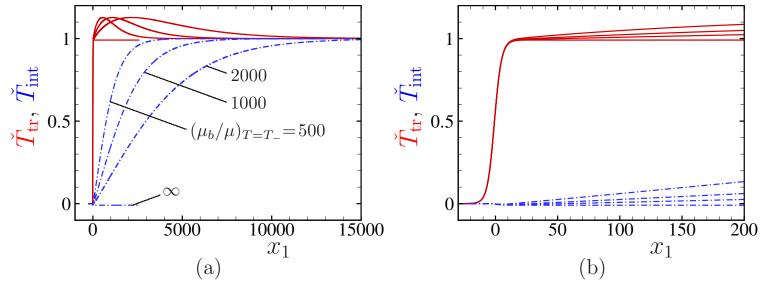

Fig. 2 Profiles of $\check{T}_{\rm tr}$ and $\check{T}_{\rm int}$ at $M_- = 1.3$ for $(\mu_b/\mu)_{T=T_-} = 500$, 1000, 2000, and ∞. (a) Profiles for $-1000 \leq x_1 \leq 15000$, (b) profiles for $-30 \leq x_1 \leq 200$. The red solid line indicates $\check{T}_{\rm tr}$ and the blue dot-dashed line $\check{T}_{\rm int}$. (Color figure online)

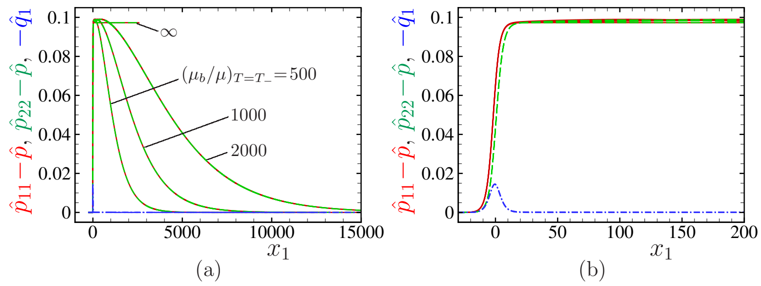

Fig. 3 Profiles of $\hat{p}_{11} - \hat{p}$, $\hat{p}_{22} - \hat{p}$, and $-\hat{q}_1$ at $M_- = 1.3$ for $(\mu_b/\mu)_{T=T_-} = 500$, 1000, 2000, and ∞. (a) Profiles for $-1000 \leq x_1 \leq 15000$, (b) profiles for $-30 \leq x_1 \leq 200$. The red solid line indicates $\hat{p}_{11} - \hat{p}$, the green dashed line $\hat{p}_{22} - \hat{p}$, and the blue dot-dashed line $-\hat{q}_1$. (Color figure online)

finity). In addition, we only show the results for large values of $(\mu_b/\mu)_{T=T_-}$, i.e., $(\mu_b/\mu)_{T=T_-} = 500$, 1000, 2000, and ∞.

In Fig. 1, we show the profiles of $\check{\rho}$, $\check{v}$, and $\check{T}$ at $M_- = 1.3$ for $(\mu_b/\mu)_{T=T_-} = 500$, 1000, 2000, and ∞. Figure 1(b) is the magnified figure of Fig. 1(a) in the range $-30 \leq x_1\ (= X_1/l_-) \leq 200$. The red solid line indicates $\check{\rho}$, the green dashed line $\check{v}$, and the blue dot-dashed line $\check{T}$ (color figure online). Note that for $(\mu_b/\mu)_{T=T_-} =$

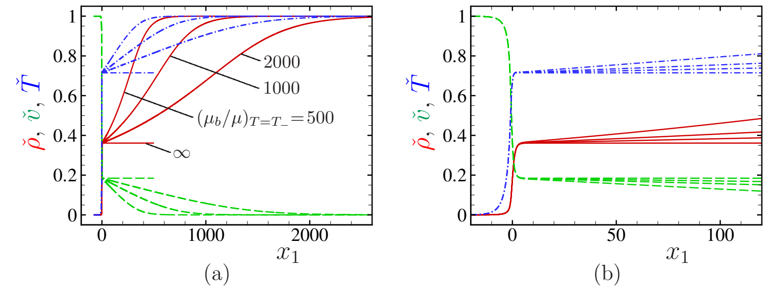

Fig. 4 Profiles of $\check{\rho}$, $\check{v}$, and $\check{T}$ at $M_- = 5$ for $(\mu_b/\mu)_{T=T_-} = 500$, 1000, 2000, and ∞. (a) Profiles for $-200 \le x_1 \le 2600$, (b) profiles for $-20 \le x_1 \le 120$. See the caption of Fig. 1. (Color figure online)

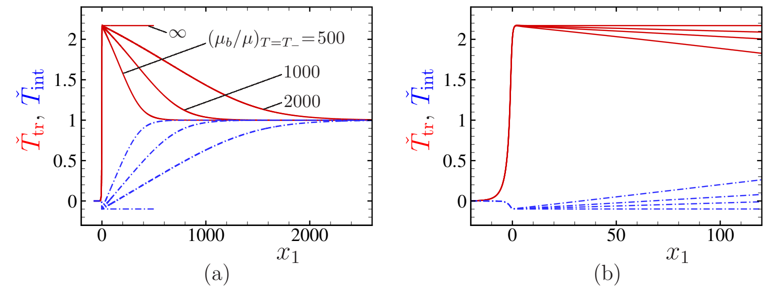

Fig. 5 Profiles of $\check{T}_{\mathrm{tr}}$ and $\check{T}_{\mathrm{int}}$ at $M_- = 5$ for $(\mu_b/\mu)_{T=T_-} = 500$, 1000, 2000, and ∞. (a) Profiles for $-200 \le x_1 \le 2600$, (b) profiles for $-20 \le x_1 \le 120$. See the caption of Fig. 2. (Color figure online)

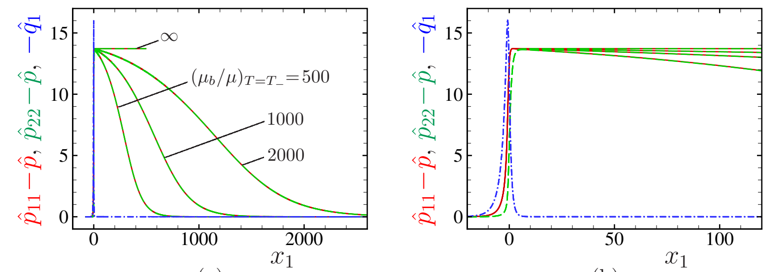

Fig. 6 Profiles of $\hat{p}_{11} - \hat{p}$, $\hat{p}_{22} - \hat{p}$, and $-\hat{q}_1$ at $M_- = 5$ for $(\mu_b/\mu)_{T=T_-} = 500$, 1000, 2000, and ∞. (a) Profiles for $-200 \le x_1 \le 2600$, (b) profiles for $-20 \le x_1 \le 120$. See the caption of Fig. 3. (Color figure online)

∞, the downstream condition is different from that for finite $(\mu_b/\mu)_{T=T_-}$ and is given by the Rankine–Hugoniot relations for $(\mu_b/\mu)_{T=T_-} = \infty$ or $\theta = 0$ [(114), (116), and (117) (note that $T_{\mathrm{tr}-} = T_{\mathrm{int}-} = T_-$ in the present problem)]. In this figure and the following Figs. 2–6, $x_1 = 0$ is set at the position where the density is equal to the average of the upstream and downstream values when $(\mu_b/\mu)_{T=T_-} = \infty$. The profiles, which are of Type C, consist of a thin front layer and a thick rear layer. As $(\mu_b/\mu)_{T=T_-}$ increases, the thickness of the rear layer increases and reaches

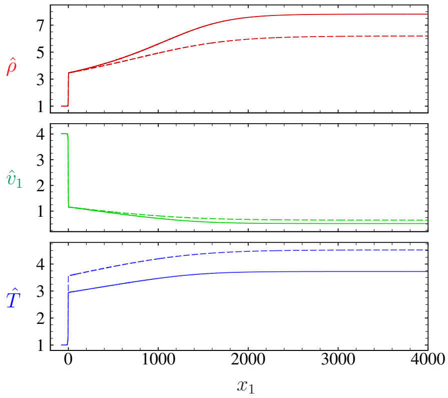

Fig. 7 Comparison of the profiles of $\hat{\rho}$, $\hat{v}_1$, and $\hat{T}$ at $M_- = 5$ for $(\mu_b/\mu)_{T=T_-} = 2000$. The solid line indicates the case of temperature-dependent specific heats (or temperature-dependent δ) and the dashed line the case of constant specific heats [or constant $\delta\,(= \delta_-)$]. The red color shows $\hat{\rho}$, the green color $\hat{v}_1$, and the blue color $\hat{T}$. (Color figure online)

over 15000 mean free paths (l_-) for $(\mu_b/\mu)_{T=T_-} = 2000$, whereas the profiles of the thin front layer are not affected by $(\mu_b/\mu)_{T=T_-}$ and coincide with the shock profiles for $(\mu_b/\mu)_{T=T_-} = \infty$.

Figure 2 shows the profiles of $\check{T}_{\mathrm{tr}}$ and $\check{T}_{\mathrm{int}}$ in the same case as Fig. 1. Figure 2(b) is the magnified figure of Fig. 2(a) in the range $-30 \le x_1 \le 200$. The red solid line indicates $\check{T}_{\mathrm{tr}}$ and the blue dot-dashed line $\check{T}_{\mathrm{int}}$ (color figure online). A significant overshoot is observed for $\check{T}_{\mathrm{tr}}$. In Fig. 3, the profiles of $\hat{p}_{11} - \hat{p}$, $\hat{p}_{22} - \hat{p}$, and $-\hat{q}_1$ are shown in the same case as Fig. 1. Figure 3(b) is the magnified figure of Fig. 3(a) in the range $-30 \le x_1 \le 200$, and the red solid line indicates $\hat{p}_{11} - \hat{p}$, the green dashed line $\hat{p}_{22} - \hat{p}$, and the blue dot-dashed line $-\hat{q}_1$ (color figure online). The $\hat{q}_1$ is nonzero only in the thin front layer and is not affected by $(\mu_b/\mu)_{T=T_-}$; $\hat{p}_{11} = \hat{p}_{22}$ holds almost whole range of the thick rear layer.

Since the temperature variation is rather small for $M_- = 1.3$ (cf. Table 1), the profiles shown in Figs. 1–3 are little affected by the temperature-dependent specific heats and almost coincide with the profiles for constant δ $(= \delta_-)$. The small difference is due to the fact that the downstream state is slightly different because of the different Rankine–Hugoniot relations (cf. Table 1).

Next, we show the profiles at a higher Mach number, $M_- = 5$, for $(\mu_b/\mu)_{T=T_-} =$ 500, 1000, 2000, and ∞. Figure 4 shows the profiles of $\check{\rho}$, $\check{v}$, and $\check{T}$, Fig. 5 those of $\check{T}_{\mathrm{tr}}$ and $\check{T}_{\mathrm{int}}$, and Fig. 6 those of $\hat{p}_{11} - \hat{p}$, $\hat{p}_{22} - \hat{p}$, and $-\hat{q}_1$. Figures 4(b), 5(b), and 6(b) are, respectively, the magnified figures of Figs. 4(a), 5(a), and 6(a) in the range $-20 \le x_1\,(= X_1/l_-) \le 120$, and the types of lines are the same as Figs. 1–3, i.e., the red solid line indicates $\check{\rho}$, the green dashed line $\check{v}$, and the blue dot-dashed line $\check{T}$ in Fig. 4; the red solid line indicates $\check{T}_{\mathrm{tr}}$ and the blue dot-dashed line $\check{T}_{\mathrm{int}}$ in Fig. 5; and the red solid line indicates $\hat{p}_{11} - \hat{p}$, the green dashed line $\hat{p}_{22} - \hat{p}$, and the blue dot-dashed line $-\hat{q}_1$ in Fig. 6 (color figure online).

In this case $(M_- = 5)$, the shock wave is thinner than that at $M_- = 1.3$ for the same $(\mu_b/\mu)_{T=T_-}$ and extend over 2600 mean free paths when $(\mu_b/\mu)_{T=T_-} =$ 2000. The change of the profiles over the thin front layer at $M_- = 5$ is steeper than that at $M_- = 1.3$. As one can see from Table 1, the values of the macroscopic quantities at downstream infinity are very different from those for a gas with constant specific heats, so that the profiles over the thick layer are significantly affected by the temperature-dependent specific heats. The profiles of $\hat{\rho}$, $\hat{v}_1$, and $\hat{T}$ are compared between the case of temperature-dependent specific heats (or temperature-dependent δ) and the case of constant specific heats [or constant δ $(= \delta_-)$] in Fig. 7 for $M_- = 5$ and $(\mu_b/\mu)_{T=T_-} = 2000$.

As was mentioned at the beginning of Sect. 3.5, the numerical method used here is essentially the same as that in [27], where the scheme and solution procedure are explained in detail (see Sects. IV B and IV C in [27]). In addition, the detailed information on the actual grid systems in x_1 and ζ_1 used in [27] is given in Appendices B 1 and B 2 in [27], and the accuracy of computation is checked in Appendix B 3 in [27]. The grid systems used for $M_- = 1.3$ in the present study is not far from those used for $M_- = 1.2$ in [27], and those used for $M_- = 5$ here is close to those for $M_- = 5$ in [27]. The accuracy of computation in the present study is almost the same as that attained for $M_- = 1.2$ and 5 in [27] (see Appendix B 3). To avoid cumbersomeness, we omit information about the data for numerical computation in the present paper.

3.6.3 Comparison with [52,53]

Now we try to compare the profiles based on the present ES model with those based on the extended thermodynamics (ET) [52,53]. The parameter setting in Sect. 3.6.1 is the same as [52] except that μ_b and λ are slightly different. In [27], it is shown that the profiles of the density, flow velocity, and temperature for $M_- = 1.47$ and $\mu_b/\mu = 5200$ obtained by using the ES model with constant specific heats agree well with those obtained in [52] (see Fig. 15 in [27] and the parameter setting there). The very small discrepancy is due to the fact that, since the specific heats of the model used in [52] are temperature dependent, the downstream equilibrium is slightly different from that of the ES model. This discrepancy is removed by the present ES model with temperature-dependent specific heats, and the two results agree perfectly. The figure of comparison for $M_- = 1.47$ and $\mu_b/\mu = 5200$ is omitted here for conciseness.

Unlike [52], the following formula of the bulk viscosity μ_b is used in [53]:

$$\mu_b = \left(\frac{2}{3} - \frac{R}{C_v}\right) p\tau, \qquad \tau = \tau_- \frac{5 - 3\gamma_-}{5 - 3\gamma(T)} \frac{\rho_-}{\rho} \left(\frac{T_-}{T}\right)^{2.3}, \tag{60}$$

where the notation in the present paper is used. In (60), $\tau = \tau(\rho, T)$ is the relaxation time for the dynamic pressure, and $\tau_- = \tau(\rho_-, T_-)$ (cf. [53]). By comparing the first equation of (60) with (27b), we obtain $\tau = 1/[\theta\rho A_c(T)]$, which leads to

$$\frac{A_c(T)}{A_c(T_-)} = \frac{5 - 3\gamma(T)}{5 - 3\gamma_-} \left(\frac{T}{T_-}\right)^{2.3}, \quad \text{or} \quad \hat{A}_c(\hat{T}) = \frac{5 - 3\gamma(\hat{T})}{5 - 3\gamma_-} \hat{T}^{2.3}. \tag{61}$$

Equation (27) with this expression gives the relations $\mu \propto [5/3 - \gamma(T)]T^{-1.3}$ and $\mu_b \propto T^{-1.3}$, which are very different from $\mu \propto T^{0.935}$ in [52]. In the comparison of the present result with the result in [53], we reset $A_c(T)$ as (61).

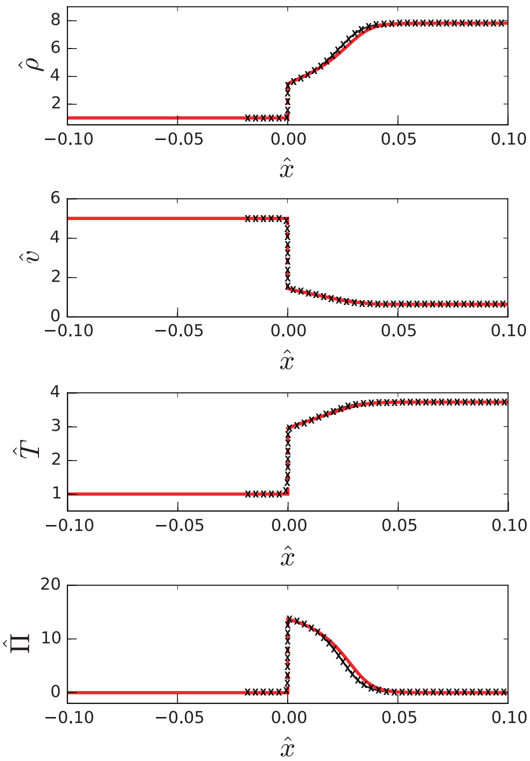

Fig. 8 Comparison between the profiles based on the present ES model and those based on the extended thermodynamics in [53]. The figure is a reproduction of Fig. 4 in [53] (courtesy of M. Sugiyama and S. Taniguchi). The profiles of $\hat{\rho}$, $\hat{v}$ (the same as our $\hat{v}_1$), $\hat{T}$, and $\hat{\Pi}$ ($= \Pi/p_-$) at $\hat{M}_- = 5$ are shown. The red thick solid line indicates the result based on the nonlinear ET6 system, and the thin black solid line that based on the linear ET6 system (see [53] for the ET6 systems); the present result based on the new ES model for $(\mu_b/\mu)_{T=T_-} = 2000$ is overdrawn by the cross symbol. (Color figure online)

We further note that the space coordinate $\hat{x}$ and the dynamic pressure Π in [53] are related to our notation as

$$\hat{x} = (8/\pi\gamma_-)^{1/2}\theta x_1, \qquad \Pi = (1/3)(p_{11} + 2p_{22}) - p. \tag{62}$$

Figure 8 shows the comparison between the present numerical solution based on the new ES model and the result based on the extended thermodynamics [53] at $\hat{M}_- = 5$. To be more specific, Fig. 8 is a reproduction of Fig. 4 in [53] with the present numerical result being overdrawn. The notations $\hat{\rho}$, $\hat{v}$, and $\hat{T}$ in the figure are the same as $\hat{\rho}$, $\hat{v}_1$, and $\hat{T}$ in the present paper, and $\hat{\Pi}$ is Π in (62) devided by p_-. In the figure, the red thick solid line indicates the result based on the nonlinear ET6 system, the thin black solid line indicates the result based on the linear ET6 system (see [53] for the ET6 systems), and the cross symbol indicates the result based on the new ES model at $(\mu_b/\mu)_{T=T_-} = 2000$ (color figure online). The latter result is shown only at discrete points to make the comparison more visible. It should be noted that with the coordinate $\hat{x}$, which is proportional to our y_1 appearing later [cf. (63)], the profiles in the thick rear layer are independent of μ_b/μ when it is large [27]. As seen from the figure, the result based on the ES model shows very good agreement with that based on the linear ET6 system. The numerical result was also compared with the results based on the nonlinear and linear ET6 systems for $M_- = 1.3$ and 3 shown in Figs. 2 and 3 in [53], where the nonlinear and linear ET6 systems give almost the same result, and very good agreement was obtained. The figure of comparison is omitted here.

In [52], the ET14 system, which is a system for 14 macroscopic variables derived on the basis of extended thermodynamics, is used, and the profiles of the macroscopic quantities are obtained in the thin front layer as well as in the thick rear layer of Type-C solution. In contrast, [53] uses the simpler ET6 system, which contains only 6 macroscopic variables, and considers its weak solution. In other words, the thin front layer is replaced by a jump (sub-shock) with a suitable jump condition [51]. In Fig. 8, this jump is indicated by the vertical dashed line, which is more visible in Fig. 4 in [53]. The result based on the new ES model describes the structure of the thin front layer, too. However, it degenerates into the vertical line in the scale of Fig. 8.

3.7 Slowly varying solution

In [27], a set of macroscopic equations that describes slow relaxation of the internal modes over the thick rear layer in Type-C solution (and the entire profiles of Type-A and B solutions) when the ratio μ_b/μ is large (i.e., θ is small) has been obtained by considering a slowly varying solution whose length scale of variation in x_1 is $1/\theta$. This system is convenient because one can obtain an analytical solution of the shock profiles. In the present section, we try to obtain the corresponding macroscopic system and its solution. Since the analysis is in parallel to Sect. V A in [27], we will make a concise description quoting [27] occasionally.

As in [27], we consider the case where $\theta \ll 1$ and introduce the space coordinates y_i:

$$y_i = (2/\sqrt{\pi})\theta x_i, \tag{63}$$

whose length scale of variation is of $O(1/\theta)$ to describe the slowly varying solution. Then, the dimensionless model equation (118) in Appendix C, which is the spatially three-dimensional version of (36), becomes (119). In Appendix C, the slowly varying solution $\hat{f}(y_i, \zeta_i, \hat{\mathscr{E}})$ is obtained in the form of expansions (120) and (121), and the macroscopic equations for the leading-order terms $\hat{\rho}^{(0)}$, $\hat{v}_j^{(0)}$, $\hat{T}_{\mathrm{tr}}^{(0)}$, and $\hat{T}_{\mathrm{int}}^{(0)}$ in expansion (121) are derived as (137) [or (138)] and one of (140) and (142).

Now we consider the spatially one-dimensional case and assume that $\partial/\partial y_2 = \partial/\partial y_3 = 0$ and $\hat{v}_2^{(0)} = \hat{v}_3^{(0)} = 0$. If we choose (137) and (142) as the governing equations and omit the superscript $^{(0)}$ for brevity, these equations reduce to the following system:

$$\frac{d}{dy_1}(\hat{\rho}\hat{v}_1) = 0, \tag{64a}$$

$$\frac{d}{dy_1}\left(\frac{\hat{T}_{\text{tr}}}{\hat{v}_1} + 2\hat{v}_1\right) = 0, \tag{64b}$$

$$\frac{d}{dy_1}\left(\hat{v}_1^2 + \frac{5}{2}\hat{T}_{\text{tr}} + \frac{\delta}{2}\hat{T}_{\text{int}}\right) = 0, \tag{64c}$$

$$\hat{v}_1\frac{d}{dy_1}(\delta\hat{T}_{\text{int}}) = \frac{3\delta}{3+\delta}\hat{A}_c(\hat{T})\hat{\rho}\left(\hat{T}_{\text{tr}} - \hat{T}_{\text{int}}\right), \tag{64d}$$

where

$$\delta = \hat{D}(\hat{T}) = \frac{2}{\hat{T}}\hat{E}(\hat{T}) - 3, \qquad \hat{T} = \hat{E}^{-1}(3\hat{T}_{\text{tr}}/2 + \delta\hat{T}_{\text{int}}/2), \tag{65}$$

[cf. (133)]; therefore the relation

$$\hat{T} = \frac{3\hat{T}_{\text{tr}} + \delta\hat{T}_{\text{int}}}{3+\delta}, \tag{66}$$

holds [cf. (143)]. Here, we have used (64a) in deriving (64b) and (64c) and used (66) in deriving (64d). Hereafter, we consider (64) supplemented by the first equation of (65) and (66) as the closed system to be solved. It should be noted that (64) is the steady version of a hyperbolic conservation system with relaxation, a simplified model of which has been studied in mathematical rigor [33].

As in Sect. V A in [27], it follows from (64a)–(64c) that [cf. (57) in [27]]

$$\hat{\rho} = \frac{c_1}{\hat{v}_1}, \qquad \hat{T}_{\text{tr}} = \hat{v}_1(c_2 - 2\hat{v}_1), \qquad \hat{T}_{\text{int}} = \frac{2}{\delta}\left(c_3 - \frac{5}{2}c_2\hat{v}_1 + 4\hat{v}_1^2\right), \tag{67}$$

where c_1, c_2, and c_3 are constants. Inserting (67) in (64d) and (66), we obtain the following equations [cf. (58) in [27]]:

$$\hat{v}_1^2\left(\frac{5}{16}c_2 - \hat{v}_1\right)\frac{d\hat{v}_1}{dy_1} = \frac{3}{8(3+\delta)}c_1\hat{A}_c(\hat{T})\left[(4+\delta)\hat{v}_1^2 - \frac{5+\delta}{2}c_2\hat{v}_1 + c_3\right], \tag{68a}$$

$$\delta = \hat{D}(\hat{T}), \qquad \hat{T} = \frac{2}{3+\delta}\left(\hat{v}_1^2 - c_2\hat{v}_1 + c_3\right). \tag{68b}$$

Since δ and $\hat{T}$ can be, in principle, expressed in terms of $\hat{v}_1$ from (68b), (68a) is the equation for $\hat{v}_1$. If we eliminate c_3 from (68a) using (68b), we have an alternative expression of (68a), i.e.,

$$\hat{v}_1^2\left(\frac{5}{16}c_2 - \hat{v}_1\right)\frac{d\hat{v}_1}{dy_1} = \frac{3}{8}c_1\hat{A}_c(\hat{T})\left(\hat{v}_1^2 - \frac{1}{2}c_2\hat{v}_1 + \frac{1}{2}\hat{T}\right). \tag{69}$$

As discussed in [27], the slowly varying solution describes either the full shock profiles (Type-A and Type-B profiles) or the profiles of the thick rear layer (Type-C profile). Therefore, $(\hat{\rho}, \hat{v}_1, \hat{T}_{\text{tr}}, \hat{T}_{\text{int}})$ should approach $(\hat{\rho}_+, \hat{v}_+, \hat{T}_+, \hat{T}_+)$ as $x_1 \to \infty$. If we consider this limit in (67), we have

$$c_1 = \hat{\rho}_+\hat{v}_+, \qquad c_2 = (\hat{T}_+/\hat{v}_+) + 2\hat{v}_+, \qquad c_3 = \hat{v}_+^2 + [(5+\delta_+)/2]\hat{T}_+. \tag{70}$$

However, the dimensionless version of (89) and the fact that $\hat{E}(1) = (3+\delta_-)/2$ and $\hat{E}(\hat{T}_+) = [(3+\delta_+)/2]\hat{T}_+$ show that the right-hand sides of three equations of (70) are equal to $\hat{v}_-$, $(1/\hat{v}_-)+2\hat{v}_-$, and $\hat{v}_-^2 + (5+\delta_-)/2$, respectively. Therefore, c_1, c_2, and c_3 are expressed, in terms of the upstream quantities, as

$$c_1 = \hat{v}_-, \qquad c_2 = \frac{1}{\hat{v}_-} + 2\hat{v}_-, \qquad c_3 = \hat{v}_-^2 + \frac{5+\delta_-}{2}. \tag{71}$$

By using (71), we can transform (69) and (68b) into the following form:

$$\hat{v}_1^2(\hat{v}_* - \hat{v}_1)\frac{d\hat{v}_1}{dy_1} = \frac{3\hat{v}_-}{8}\hat{A}_c(\hat{T})\left(\hat{v}_1^2 - \frac{1+2\hat{v}_-^2}{2\hat{v}_-}\hat{v}_1 + \frac{1}{2}\hat{T}\right), \tag{72a}$$

$$\delta = \hat{D}(\hat{T}), \tag{72b}$$

$$\hat{T} = \frac{2}{3+\delta}\left[\frac{3+\delta_-}{2} + (\hat{v}_1 - \hat{v}_-)\left(\hat{v}_1 - \frac{1+\hat{v}_-^2}{\hat{v}_-}\right)\right], \tag{72c}$$

where

$$\hat{v}_* = \frac{5}{16}\frac{1+2\hat{v}_-^2}{\hat{v}_-}, \tag{73}$$

and we should recall that $\delta_- = \hat{D}(1)$. When $\hat{v}_1 = \hat{v}_-$, (72c) shows that $\hat{E}(\hat{T}) = [(3+\delta)/2]\hat{T} = (3+\delta_-)/2 = \hat{E}(1)$, so that $\hat{T} = 1$ and thus $\delta = \delta_-$. In this case, it is readily seen that the right-hand side of (72a) vanishes. Therefore, $\hat{v}_1 = \hat{v}_-$ is an equilibrium point of (72a) if $\hat{v}_* \neq \hat{v}_-$. On the other hand, if we use (70) in (68), we obtain (72a) and (72c) with alternative expressions of the right-hand sides in terms of the downstream quantities δ_+ $[= \hat{D}(\hat{T}_+)]$, $\hat{v}_+$, and $\hat{T}_+$ [and $\hat{\rho}_+$ for (72a)]. From these expressions, we can readily see that when $\hat{v}_1 = \hat{v}_+$, it follows that $\hat{T} = \hat{T}_+$ and thus $\delta = \delta_+$. Therefore, it is easy to see that the right-hand side of (72a) vanishes at $\hat{v}_1 = \hat{v}_+$, that is, it is an equilibrium point of (72a) if $\hat{v}_* \neq \hat{v}_+$. The (local) stability of the equilibrium points is discussed in Appendix D.

Once $\hat{v}_1$ is obtained from (72), other quantities follow from (67) with (71), i.e.,

$$\hat{\rho}(\hat{v}_1) = \frac{\hat{v}_-}{\hat{v}_1}, \qquad \hat{T}_{\mathrm{tr}}(\hat{v}_1) = 1 + 2(\hat{v}_- - \hat{v}_1)\left(\hat{v}_1 - \frac{1}{2\hat{v}_-}\right), \tag{74a}$$

$$\hat{T}_{\mathrm{int}}(\hat{v}_1) = \frac{\delta_-}{\delta} + \frac{8}{\delta}(\hat{v}_1 - \hat{v}_-)(\hat{v}_1 - \hat{v}_{**}), \tag{74b}$$

where

$$\hat{v}_{**} = \frac{5+2\hat{v}_-^2}{8\hat{v}_-}, \tag{75}$$

which is the dimensionless downstream velocity of the shock wave when $\theta = 0$ corresponding to v_+ in (114a). When $\hat{v}_1 = \hat{v}_-$, we have $\hat{\rho} = \hat{T}_{\mathrm{tr}} = \hat{T}_{\mathrm{int}} = 1$ because $\delta = \delta_-$. Similarly, from the alternative expressions of $\hat{\rho}$, $\hat{T}_{\mathrm{tr}}$, and $\hat{T}_{\mathrm{int}}$ obtained by using (70) in (67), it is seen that when $\hat{v}_1 = \hat{v}_+$, we have $\hat{\rho} = \hat{\rho}_+$ and $\hat{T}_{\mathrm{tr}} = \hat{T}_{\mathrm{int}} = \hat{T}_+$.

Since (72) is more implicit than the corresponding equation, (60) in [27], in the case of constant δ, we can obtain less information about the global behavior of the solution. However, according to the stability analysis in Appendix D, we can expect the basic properties of (60) in [27] are retained in (72). Therefore, we try to integrate it in the similar way as in [27]. From (72a), we obtain

$$\frac{dy_1}{d\hat{v}_1} = \frac{8}{3\hat{v}_-} \frac{\hat{v}_1^2(\hat{v}_* - \hat{v}_1)}{\hat{A}_c(\hat{T})\left(\hat{v}_1^2 - \frac{1+2\hat{v}_-^2}{2\hat{v}_-}\hat{v}_1 + \frac{1}{2}\hat{T}\right)}. \tag{76}$$

Assuming that $\hat{v}_1$ is a decreasing function of y_1, we integrate (76) from $\hat{v}_1$ to $\hat{v}_0$ to obtain

$$y_1(\hat{v}_1) - y_0 = -\frac{8}{3\hat{v}_-}\int_{\hat{v}_1}^{\hat{v}_0} \frac{u^2(\hat{v}_* - u)}{\hat{A}_c(\hat{T})\left(u^2 - \frac{1+2\hat{v}_-^2}{2\hat{v}_-}u + \frac{1}{2}\hat{T}\right)} du, \tag{77}$$

where

$$\delta = \hat{D}(\hat{T}), \tag{78a}$$

$$\hat{T} = \frac{2}{3+\delta}\left[\frac{3+\delta_-}{2} + (u - \hat{v}_-)\left(u - \frac{1+\hat{v}_-^2}{\hat{v}_-}\right)\right], \tag{78b}$$

and $y_0 = y_1(\hat{v}_0)$. The inverse function of $y_1(\hat{v}_1)$ gives the velocity profile $\hat{v}_1(y_1)$ with the initial condition $\hat{v}_1 = \hat{v}_0$ at $y_1 = y_0$.

As in [27], we can make the following settings of y_0 and $\hat{v}_0$ depending on the upstream Mach number M_- as well as the effective upstream Mach number $\widetilde{M}_-$ for $\theta = 0$ that is defined by (114b) in Appendix B.2 (note that $T_{\mathrm{tr}-} = T_-$ in the present problem; see also Appendix D):

(i) For $\widetilde{M}_- < 1 < M_-$, we let $y_0 = -\infty$ and $\hat{v}_0 = \hat{v}_-$. Then, the resulting profiles of $\hat{v}_1(y_1)$ and other macroscopic quantities exhibit the entire profiles of Type A.

(ii) For $1 < \widetilde{M}_-(< M_-)$, we let $y_0 = 0$ and $\hat{v}_0 = \hat{v}_{**}$ defined by (75). Then, the resulting profiles of $\hat{v}_1(y_1)$ and other macroscopic quantities demonstrate the profiles in the thick rear layer of Type-C solution.

(iii) For $\widetilde{M}_- = 1(< M_-)$, we let $y_0 = 0$ and $\hat{v}_0 = \hat{v}_-$. Then, the profiles of $\hat{v}_1(y_1)$ and other macroscopic quantities show the entire profiles of Type B with a corner at the start of the profiles $y_1 = 0$.

Now we compare the solution (77) in case (ii) (Type-C profile) with the numerical results that were shown in Figs. 1, 2, 4, and 5. Figures 9(a) and 9(b) are, respectively, the same as Figs. 1(a) and 2(a) for $M_- = 1.3$, but y_1 is used instead of x_1. Therefore, the curves for $(\mu_b/\mu)_{T=T_-} = 500$, 1000, and 2000 coincide except in the thin front layer. The result obtained from (77) is shown by the cross symbol at discrete points of y_1 to make the comparison clear. Figures 10(a) and 10(b) are, respectively, the same as Figs. 4(a) and 5(a) for $M_- = 5$, and the manner of comparison is the same as in Fig. 9. The figures show perfect agreement between the solution based on (77) and numerical solution using the new ES model.

As remarked at the end of Appendix C.2, the macroscopic equations used here are essentially the same as the ET6 system that has been used to analyze the shock-wave structure in [51,53,40]. In these references, to describe the Type-C profile,

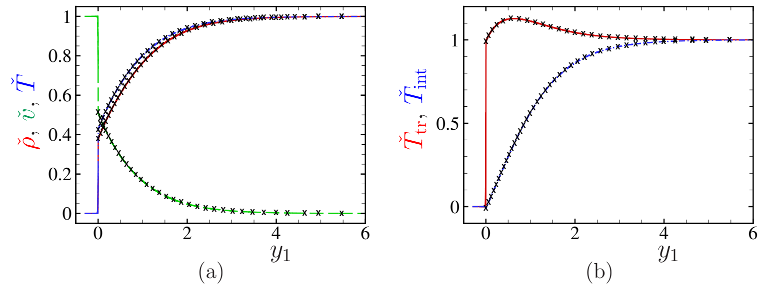

Fig. 9 Comparison between the profiles based on the slowly varying solution and those based on the numerical solution at $M_- = 1.3$. (a) Profiles of $\check{\rho}$, $\check{v}$, and $\check{T}$, (b) profiles of $\check{T}_{tr}$ and $\check{T}_{int}$. The cross symbol indicates the slowly varying solution, and the curves indicate the numerical solution for $(\mu_b/\mu)_{T=T_-} = 500$, 1000, and 2000. See Figs. 1(a) and 2(a) and the captions of Figs. 1 and 2

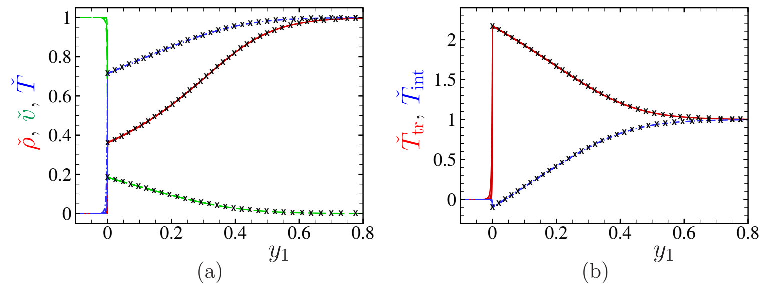

Fig. 10 Comparison between the profiles based on the slowly varying solution and those based on the numerical solution at $M_- = 5$. (a) Profiles of $\check{\rho}$, $\check{v}$, and $\check{T}$, (b) profiles of $\check{T}_{tr}$ and $\check{T}_{int}$. See the caption of Fig. 9

the weak solution of the ET6 system has been considered, that is, a sub-shock with an appropriate jump condition is set and is connected with the solution of ET6 system. In the present section, as well as Sect. V in [27], we identified the thin front layer of the Type-C profile as the shock wave for $\theta = 0$ (or infinitely large μ_b/μ) numerically and combined (64) with the corresponding Rankine–Hugoniot relations to describe the Type-C profile. Since (64) is derived under the slowly varying assumption, the weak solution, which allows discontinuities, should be excluded. However, if we admit (64) as the basic equation, we can proceed in the same way as in the case of the ET6 system. It should also be mentioned that shock-wave structure for CO_2 gas was studied recently by using different continuum models, including the Navier–Stokes equations [1].

4 Concluding remarks

In the present study, we have proposed a new kinetic model for the Boltzmann equation for a polyatomic gas with temperature-dependent specific heats (thermally perfect gas or non-polytropic gas) (Sect. 2.1). It is a straightforward extension of the conventional ES model for a gas with constant specific heats (calorically perfect gas or polytropic gas) [2, 14]. The basic properties of the new model, such as the equilibrium solution, the conservation laws, and the H theorem (only in the space-homogeneous case), have been established (Sect. 2.2). The formulas of the viscosity, bulk viscosity, and thermal conductivity were also derived via the Chapman–Enskog expansion (Sect. 2.3).

Then, the model was applied to the problem of the shock-wave structure of CO_2 gas, which is known to have a very large value of the ratio of the bulk viscosity to the viscosity (Sect. 3). First, the problem was tackled by a direct numerical analysis taking the advantage of the fact that the model can be reduced to a system of three integro-differential equations with only two independent variables (Sects. 3.4 and 3.5). The numerical analysis was carried out in parallel to the case of a gas with constant specific heats [27]. The detailed profiles of macroscopic quantities across the shock wave have been shown for two typical upstream Mach numbers ($M_- = 1.3$ and 5) that provides the Type-C profile defined in [52] (i.e., the profile consisting of a thin front layer with rapid change and a thick rear layer with slow relaxation) (Sect. 3.6). In the case of the higher Mach number ($M_- = 5$), the effect of the temperature dependence of the specific heats has a large effect, and the profiles are significantly different from those for the gas with constant specific heats. The results were also compared with those based on the extended thermodynamics [53], and very good agreement was shown.

Following the analysis in [27], we also considered the case where the ratio of the bulk viscosity to the viscosity is large and derived a system of macroscopic equations for the slowly varying solution, which describes the slow relaxation of the internal modes, using a Hilbert-type expansion (Sect. 3.7). The system, which is an extension of the system derived in [27] to the case of temperature-dependent specific heats, is the steady version of a hyperbolic system with relaxation and is basically the same as the system called ET6 in [53]. The numerical computation based on the analytical solution of this system, combined with the Rankine–Hugoniot relations for infinitely large bulk viscosity, gives the profiles of the thick rear layer of Type-C profile in perfect agreement with the numerical solution of the new ES model shown in Sect. 3.6.

In the present paper, the shock structure was compared only with that based on the extended thermodynamics. The comparison with the results using other models and other numerical approaches, such as DSMC, would be of interest and importance. In addition, we showed only one example of application of the new ES model for a gas with temperature-dependent specific heats. Different applications, such as spatially multi-dimensional flow problems containing shock waves, would be an interesting future problem.

Acknowledgements The authors thank Professor Masaru Sugiyama for valuable comments and professor Shigeru Taniguchi for providing an original figure of his paper. One of the authors (K.A.) thanks Department of Mathematics, National Cheng Kung University and National Center for Theoretical Sciences, National Taiwan University for their support and hospitality.

A Basic properties for $\theta = 0$

In this appendix, we summarize the basic properties corresponding to Propositions 1 and 2 when $\theta = 0$ and give some comments on Propositions 3 and 4 in this case.

Proposition 1′ (conservation for $\theta = 0$): For an arbitrary function $f(t, \boldsymbol{X}, \boldsymbol{\xi}, \mathscr{E})$, the following relation holds:

$$\iint_0^\infty \varphi_r Q(f) d\mathscr{E} d\boldsymbol{\xi} = 0, \tag{79}$$

where φ_r ($r = 0, ..., 5$) are the collision invariants, i.e.,

$$\varphi_0 = 1, \qquad \varphi_i = \xi_i \quad (i = 1, 2, 3), \qquad \varphi_4 = \frac{1}{2}|\boldsymbol{\xi}|^2, \qquad \varphi_5 = \mathscr{E}. \tag{80}$$

Proposition 2′ (equilibrium for $\theta = 0$): The vanishing of the collision term $Q(f) = 0$ is equivalent to the fact that f is the following local equilibrium distribution:

$$f_{\mathrm{eq}} = \frac{\bar{\rho}\mathscr{E}^{\bar{\delta}/2-1}}{(2\pi R\bar{T}_{\mathrm{tr}})^{3/2}(R\bar{T}_{\mathrm{int}})^{\bar{\delta}/2}\Gamma(\bar{\delta}/2)} \exp\left(-\frac{|\boldsymbol{\xi} - \bar{\boldsymbol{v}}|^2}{2R\bar{T}_{\mathrm{tr}}} - \frac{\mathscr{E}}{R\bar{T}_{\mathrm{int}}}\right), \tag{81}$$

where $\bar{\rho}$, $\bar{\boldsymbol{v}}$, $\bar{T}_{\mathrm{tr}}$, and $\bar{T}_{\mathrm{int}}$ are arbitrary functions of t and $\boldsymbol{X}$, and $\bar{\delta}$ and $\bar{T}$ are determined by the following coupled equations:

$$\bar{\delta} = D(\bar{T}), \qquad \bar{T} = E^{-1}(3R\bar{T}_{\mathrm{tr}}/2 + \bar{\delta}R\bar{T}_{\mathrm{int}}/2). \tag{82}$$

The solution $(\bar{\delta}, \bar{T})$ of (82) exists. In particular, it is unique when $\bar{T}_{\mathrm{int}} \le \bar{T}_{\mathrm{tr}}$.

Proof of Proposition 1′: As is seen from (20a) and (21a), (79) holds for $\varphi_0 = 1$ and $\varphi_r = \xi_r$ ($r = 1, 2, 3$) also for $\theta = 0$. Because $T_{\mathrm{rel}} = T_{\mathrm{int}}$ when $\theta = 0$, (21a) and (21b) reduce to

$$\iint_0^\infty \xi_k^2 \mathscr{G} d\mathscr{E} d\boldsymbol{\xi} = 3R\rho T_{\mathrm{tr}} + \rho v_k^2 = 2\rho e_{\mathrm{tr}} + \rho v_k^2, \qquad \iint_0^\infty \mathscr{E}\mathscr{G} d\mathscr{E} d\boldsymbol{\xi} = \rho\frac{\delta R T_{\mathrm{int}}}{2} = \rho e_{\mathrm{int}}. \tag{83}$$

Therefore, instead of (16) with $\varphi_4 = |\boldsymbol{\xi}|^2/2 + \mathscr{E}$, the following relations hold independently:

$$\iint_0^\infty \xi_k^2 (\mathscr{G} - f) d\mathscr{E} d\boldsymbol{\xi} = 0, \qquad \iint_0^\infty \mathscr{E}(\mathscr{G} - f) d\mathscr{E} d\boldsymbol{\xi} = 0, \tag{84}$$

that is, (79) holds with $r = 4$ and 5. $\square$

Proof of Proposition 2′: First, we discuss the coupled equations (82). From (4) and (82), it follows that

$$E(\bar{T}) = \frac{3}{2}R\bar{T}_{\mathrm{tr}} + \frac{D(\bar{T})}{2}R\bar{T}_{\mathrm{int}} = \frac{3}{2}R(\bar{T}_{\mathrm{tr}} - \bar{T}_{\mathrm{int}}) + \frac{\bar{T}_{\mathrm{int}}}{\bar{T}}E(\bar{T}). \tag{85}$$

If $\bar{T}_{\mathrm{tr}} = \bar{T}_{\mathrm{int}}$, then there is a unique solution $\bar{T} = \bar{T}_{\mathrm{tr}} = \bar{T}_{\mathrm{int}}$. Therefore, we assume $\bar{T}_{\mathrm{tr}} \neq \bar{T}_{\mathrm{int}}$ in the following. Then, we have

$$E(\bar{T}) = \frac{3}{2}R(\bar{T}_{\mathrm{tr}} - \bar{T}_{\mathrm{int}})\frac{\bar{T}}{\bar{T} - \bar{T}_{\mathrm{int}}}. \tag{86}$$

If we denote the right-hand side of this equation by $f(\bar{T})$, then

$$f'(\bar{T}) = \frac{3}{2}R\frac{\bar{T}_{\mathrm{int}}(\bar{T}_{\mathrm{int}} - \bar{T}_{\mathrm{tr}})}{(\bar{T} - \bar{T}_{\mathrm{int}})^2}. \tag{87}$$

(i) When $\bar{T}_{\mathrm{tr}} > \bar{T}_{\mathrm{int}}$, $f(\bar{T})$ is monotonically decreasing and has the following properties:

$$f(\bar{T}) < 0 \quad (0 < \bar{T} < \bar{T}_{\mathrm{int}}), \qquad f(\bar{T}_{\mathrm{int}} - 0) = -\infty, \qquad f(\bar{T}_{\mathrm{int}} + 0) = +\infty,$$
$$f(\bar{T}_{\mathrm{tr}}) = \frac{3}{2}R\bar{T}_{\mathrm{tr}}, \qquad f(+\infty) = \frac{3}{2}R(\bar{T}_{\mathrm{tr}} - \bar{T}_{\mathrm{int}}).$$

From this and the fact that $E(\bar{T})$ is monotonically increasing and $E(\bar{T}_{\mathrm{tr}}) > 3R\bar{T}_{\mathrm{tr}}/2$, we conclude that $\bar{T} \in (\bar{T}_{\mathrm{int}}, \bar{T}_{\mathrm{tr}})$ satisfying (86) is determined uniquely.

(ii) When $\bar{T}_{\rm tr} < \bar{T}_{\rm int}$, $f(\bar{T})$ is monotonically increasing and has the following properties:

$$f(\bar{T}) > 0 \quad (0 < \bar{T} < \bar{T}_{\rm int}), \qquad f(\bar{T}_{\rm tr}) = \frac{3}{2}R\bar{T}_{\rm tr}, \qquad f(\bar{T}_{\rm int} - 0) = +\infty,$$
$$f(\bar{T}_{\rm int} + 0) = -\infty, \qquad f(+\infty) = -\frac{3}{2}R(\bar{T}_{\rm int} - \bar{T}_{\rm tr}).$$

Since $E(\bar{T}_{\rm tr}) > 3R\bar{T}_{\rm tr}/2$ and $E(\bar{T}_{\rm int})$ is finite, there exist at least one $\bar{T} \in (\bar{T}_{\rm tr}, \bar{T}_{\rm int})$ satisfying (86). However, there is a possibility of multiple solutions depending on the functional form of $E(\bar{T})$. If there are two sets of solutions $(\bar{T}_1, \bar{\delta}_1)$ and $(\bar{T}_2, \bar{\delta}_2)$, i.e.,

$$\bar{\delta}_1 = D(\bar{T}_1), \qquad \bar{T}_1 = E^{-1}\left(3R\bar{T}_{\rm tr}/2 + \bar{\delta}_1 R\bar{T}_{\rm int}/2\right),$$
$$\bar{\delta}_2 = D(\bar{T}_2), \qquad \bar{T}_2 = E^{-1}\left(3R\bar{T}_{\rm tr}/2 + \bar{\delta}_2 R\bar{T}_{\rm int}/2\right),$$

then $\bar{T}_1 \neq \bar{T}_2$ is equivalent to $\bar{\delta}_1 \neq \bar{\delta}_2$ because the correspondence between T and e by $T = E^{-1}(e)$ is unique. In other words, if there are two sets of solutions, there is no possibility that only one of $\bar{T}$ and $\bar{\delta}$ is different.

Now we go back to the original problem. We choose a set $(\bar{T}, \bar{\delta})$ satisfying (82) and construct $f_{\rm eq}$ according to (81). We first show that if $f = f_{\rm eq}$, then $Q(f) = 0$, i.e., $\mathscr{G} = f_{\rm eq} = f$. Equations (8d) and (9) with this f give $p_{ij} = R\bar{\rho}\bar{T}_{\rm tr}\delta_{ij}$, $e_{\rm tr} = 3R\bar{T}_{\rm tr}/2$, $e_{\rm int} = \bar{\delta}R\bar{T}_{\rm int}/2$, and $e = 3R\bar{T}_{\rm tr}/2 + \bar{\delta}R\bar{T}_{\rm int}/2$. This e and (8e) uniquely determine δ, which is the same as $\bar{\delta}$ $(\delta = \bar{\delta})$ used in the construction of $f_{\rm eq}$. This is due to the following fact. Since the right-hand side of the first equation of (8e) is the same as that of the second equation of (82), the T obtained from the first equation of (8e) is the same as $\bar{T}$. Therefore, from the argument in (ii) above, it is concluded that the δ determined from the second equation of (8e) cannot be different from $\bar{\delta}$. Then, noting that $\theta = 0$, we obtain $\mathsf{T}_{ij} = R\bar{T}_{\rm tr}\delta_{ij}$, which gives $\det(\mathsf{T}) = (R\bar{T}_{\rm tr})^3$, from (8b) and $T_{\rm rel} = \bar{T}_{\rm int}$ from (8f). Consequently, it is shown that $\mathscr{G} = f_{\rm eq}$ $(= f)$.

Next, we show that if $Q(f) = 0$, f must be of the form of (81). Suppose that $f = \mathscr{G}$ for an arbitrarily given f, where $\mathscr{G}$ is constructed from f with the help of (8) and (9). Then, from (8d) and (9) with $f = \mathscr{G}$ and from (21a) and (21b), we obtain $p_{ij} = \rho(\mathsf{T})_{ij}$, $e_{\rm tr} = (\mathsf{T})_{kk}/2$, and $e_{\rm int} = \delta RT_{\rm int}/2$. Since $\nu \neq 1$, (8b) gives $(\mathsf{T})_{ij} = RT_{\rm tr}\delta_{ij}$. In this case, since $e = e_{\rm tr} + e_{\rm int} = 3RT_{\rm tr}/2 + \delta RT_{\rm int}/2$, the (T, δ) obtained by (8e) is the solution of (82). On the other hand, $\det(\mathsf{T}) = (RT_{\rm tr})^3$ and $(\mathsf{T}^{-1})_{ij} = \delta_{ij}/RT_{\rm tr}$ hold. Therefore, $\mathscr{G}$ is reduced to a function of the form of (81). In other words, f must be of the form of $f_{\rm eq}$. □

We conclude this appendix noting that Propositions 3 and 4 hold also in the case of $\theta = 0$. The only difference is that the equality sign holds for $f_{\rm eq}$ given by (81).

B Rankine–Hugoniot relations

In this appendix, we first derive the Rankine–Hugoniot relations in the case of $\theta \neq 0$, which are summarized as Proposition 5. Then, the derivation is also made in the case of $\theta = 0$.

B.1 Rankine–Hugoniot relations for $\theta \neq 0$ (Proof of Proposition 5)

Multiplying (6) (with $\partial f/\partial t = \partial f/\partial X_2 = \partial f/\partial X_3 = 0$) by $(1, \xi_i, |\boldsymbol{\xi}|^2/2 + \mathscr{E})$, integrating the resulting equations with respect to $\boldsymbol{\xi}$ over its whole space and $\mathscr{E}$ from 0 to ∞, and taking (16) and (20) into account, we obtain

$$\rho v_1 = \text{const}, \qquad p_{1i} + \rho v_1 v_i = \text{const} \quad (i = 1, 2, 3), \tag{88a}$$

$$q_1 + p_{1k}v_k + v_1\left(\rho e + \frac{1}{2}\rho|\boldsymbol{v}|^2\right) = \text{const}. \tag{88b}$$

If we apply (88) between the upstream and downstream equilibrium states and note that $\boldsymbol{v}_\pm = (v_\pm, 0, 0)$, $(p_{ij})_\pm = p_\pm \delta_{ij} = R\rho_\pm T_\pm \delta_{ij}$, and $(q_i)_\pm = 0$, we obtain the following relations:

$$\rho_- v_- = \rho_+ v_+, \tag{89a}$$

$$R\rho_- T_- + \rho_- v_-^2 = R\rho_+ T_+ + \rho_+ v_+^2, \tag{89b}$$

$$\rho_- v_- \left(RT_- + E(T_-) + \frac{1}{2} v_-^2 \right) = \rho_+ v_+ \left(RT_+ + E(T_+) + \frac{1}{2} v_+^2 \right). \tag{89c}$$

We first try to obtain T_+. If we divide (89c) by (89a) and let $d_E(T) = E(T) - E(T_-)$, we obtain

$$RT_- + \frac{1}{2} v_-^2 = RT_+ + d_E(T_+) + \frac{1}{2} v_+^2. \tag{90}$$

Multiplying this equation by $2\rho_+$, subtracting (89b), and interchanging the left- and right-hand sides, we have

$$\rho_+ \left[RT_+ + 2d_E(T_+) \right] = \rho_+ \left(2RT_- + v_-^2 \right) - \rho_- \left(RT_- + v_-^2 \right). \tag{91}$$

By multiplying by v_+ and using (89a), this relation is transformed into

$$RT_+ + 2d_E(T_+) - \left(2RT_- + v_-^2 \right) = - \left(\frac{RT_-}{v_-} + v_- \right) v_+. \tag{92}$$

If we square both sides of (92) and eliminate v_+^2 using (90), we obtain the following equation:

$$\begin{aligned} (RT_+)^2 + 2RT_+ \left[2d_E(T_+) + \left(\frac{RT_-}{v_-} \right)^2 \right] \\ + \left[2d_E(T_+) - 2RT_- - v_-^2 \right] \left[2d_E(T_+) + \left(\frac{RT_-}{v_-} \right)^2 \right] = 0. \end{aligned} \tag{93}$$

We use the symbols M_-, γ_-, and τ defined in (30) and (31) and the following dimensionless quantities:

$$\hat{d}_E(\hat{T}) = \frac{d_E(T)}{RT_-} = \int_{T_-}^{T} \frac{C_v(s)}{RT_-} ds = \int_1^{\hat{T}} \hat{C}_v(\hat{s}) d\hat{s}, \tag{94a}$$

$$\hat{T} = \frac{T}{T_-}, \qquad \hat{C}_v(\hat{T}) = \frac{C_v(T_- \hat{T})}{R}. \tag{94b}$$

The symbols $\hat{T}$ and $\hat{C}_v$ appear in (35). Then, (93), divided by $(RT_-)^2$, leads to

$$\tau^2 + 2\tau \left[2\hat{d}_E(\tau) + \frac{1}{\gamma_- M_-^2} \right] + \left[2\hat{d}_E(\tau) - 2 - \gamma_- M_-^2 \right] \left[2\hat{d}_E(\tau) + \frac{1}{\gamma_- M_-^2} \right] = 0. \tag{95}$$

Since $\tau > 0$, we can formally solve (95) to obtain

$$\tau = - \left(2\hat{d}_E(\tau) + \frac{1}{\gamma_- M_-^2} \right) + \left(\frac{1}{\sqrt{\gamma_-} M_-} + \sqrt{\gamma_-} M_- \right) \sqrt{2\hat{d}_E(\tau) + \frac{1}{\gamma_- M_-^2}}. \tag{96}$$

Because $\hat{d}_E(1) = 0$, $\tau = 1$ is a solution.

In order to consider if there is a nontrivial solution $\tau > 1$, we define the function $f(x)$ by

$$f(x) = - \left(2\hat{d}_E(x) + \frac{1}{\gamma_- M_-^2} \right) + \left(\frac{1}{\sqrt{\gamma_-} M_-} + \sqrt{\gamma_-} M_- \right) \sqrt{2\hat{d}_E(x) + \frac{1}{\gamma_- M_-^2}}, \tag{97}$$

and examine if the curves $y = f(x)$ and $y = x$ intersect at x larger than $x = 1$ (obviously they intersect at $x = 1$). From

$$f'(x) = -2\hat{C}_v(x)\left(1 - \frac{1+\gamma_- M_-^2}{2\sqrt{2\gamma_- M_-^2 \hat{d}_E(x)+1}}\right), \tag{98}$$

we have, for $M_- > 1$,

$$f'(1) = \hat{C}_v(1)\left(\gamma_- M_-^2 - 1\right) > \frac{C_v(T_-)}{R}\left(\frac{C_v(T_-)+R}{C_v(T_-)} - 1\right) = 1. \tag{99}$$

On the other hand, since we assumed that $C_v > 3R/2$, we have $\hat{d}_E(x) > (3/2)(x-1)$. Therefore, if we take a sufficiently large constant K, we can make

$$1 - \frac{1+\gamma_- M_-^2}{2\sqrt{2\gamma_- M_-^2 \hat{d}_E(x)+1}} > \frac{1}{2}, \quad \text{for } x \geq K, \tag{100}$$

so that

$$f'(x) < -\hat{C}_v(x) < -\frac{3}{2}, \qquad \text{for } x \geq K. \tag{101}$$

From this, it follows that

$$f(x) < f(K) - \frac{3}{2}\int_K^x dx = -\frac{3}{2}x + f(K) + \frac{3}{2}K. \tag{102}$$

To summarize, the curve $y = f(x)$ intersects $y = x$ at $x = 1$ and once goes above it for $x > 1$ because of (99). However, since $y = f(x)$ decreases indefinitely as x for $x > K$, it intersects $y = x$ at least one more time. Therefore, a nontrivial solution $\tau > 1$ of (95) exists. If $\hat{C}_v(x)$ is a monotonically increasing function, $f'(x)$ is a strictly decreasing function because $\hat{d}_E(x)$ is a strictly increasing function. Therefore, the curve $y = f(x)$ is convex upward and intersects $y = x$ only once for $x > 1$. In this case, the nontrivial solution $\tau > 1$ is unique.

We assume that the nontrivial solution $\tau = T_+/T_-$ has been obtained and try to obtain v_+. If we divide (92) by RT_- and make use of (30), we have

$$\tau + 2\hat{d}_E(\tau) - \left(2 + \gamma_- M_-^2\right) = -\left(1 + \gamma_- M_-^2\right)\frac{v_+}{v_-}. \tag{103}$$

With the help of (96), this is transformed as

$$\frac{v_+}{v_-} = \frac{2 + \gamma_- M_-^2 - \tau - 2\hat{d}_E(\tau)}{1 + \gamma_- M_-^2} = \frac{1 + \gamma_- M_-^2 - \sqrt{2\gamma_- M_-^2 \hat{d}_E(\tau) + 1}}{\gamma_- M_-^2}. \tag{104}$$

From (89a), we have

$$\frac{\rho_+}{\rho_-} = \frac{v_-}{v_+}. \tag{105}$$

Obviously, when $\tau = T_+/T_- = 1$, it follows from (104) and (105) that $\rho_+/\rho_- = v_+/v_- = 1$. The discussion given above completes the proof of Proposition 5.

If C_v is constant and of the form $C_v = (3+\delta)R/2$ with a constant δ, then γ is constant, and $\hat{d}_E(\tau)$ becomes

$$\hat{d}_E(\tau) = \frac{3+\delta}{2}(\tau - 1) = \frac{1}{\gamma - 1}(\tau - 1). \tag{106}$$

Using this in (95) and (104) and carrying out some algebra, we obtain the following relations:

$$\frac{T_+}{T_-} = \frac{\left[2\gamma M_-^2 - (\gamma - 1)\right]\left[(\gamma - 1)M_-^2 + 2\right]}{(\gamma + 1)^2 M_-^2}, \qquad \frac{v_+}{v_-} = \frac{(\gamma - 1)M_-^2 + 2}{(\gamma + 1)M_-^2}. \tag{107}$$

Equations (105) and (107) are nothing but the Rankine–Hugoniot relations when C_v and C_p (thus γ) are constant.

B.2 Rankine–Hugoniot relations for $\theta = 0$

If we Multiply (6) (with $\partial f/\partial t = \partial f/\partial X_2 = \partial f/\partial X_3 = 0$) by $(1, \xi_i, |\boldsymbol{\xi}|^2/2, \mathscr{E})$, integrate the resulting equations with respect to $\boldsymbol{\xi}$ over its whole space and $\mathscr{E}$ from 0 to ∞, and take (79) and (20) into account, we obtain

$$\rho v_1 = \text{const}, \qquad p_{1i} + \rho v_1 v_i = \text{const} \quad (i = 1, 2, 3), \tag{108a}$$

$$(q_{\text{tr}})_1 + p_{1k} v_k + v_1 \left(\rho e_{\text{tr}} + \frac{1}{2} \rho |\boldsymbol{v}|^2 \right) = \text{const}, \tag{108b}$$

$$(q_{\text{int}})_1 + \rho v_1 e_{\text{int}} = \text{const}, \tag{108c}$$

where

$$(q_{\text{tr}})_i = \iint_0^\infty \frac{1}{2} (\xi_i - v_i) |\boldsymbol{\xi} - \boldsymbol{v}|^2 f d\mathscr{E} d\boldsymbol{\xi}, \qquad (q_{\text{int}})_i = \iint_0^\infty (\xi_i - v_i) \mathscr{E} f d\mathscr{E} d\boldsymbol{\xi}. \tag{109}$$

On the other hand, the equilibrium distributions at upstream and downstream infinities are given on the basis of (81). Therefore, one can specify four constants $(\rho_-, v_-, T_{\text{tr}-}, T_{\text{int}-})$ at upstream infinity when $\theta = 0$ instead of the three (ρ_-, v_-, T_-). Accordingly, the downstream constant $(\rho_+, v_+, T_{\text{tr}+}, T_{\text{int}+})$ should be determined by appropriate relations (Rankine–Hugoniot relation). We will obtain this relation. The equilibrium distributions at upstream and downstream infinities can be expressed as

$$f = \frac{\rho_- \mathscr{E}^{\delta_-/2-1}}{(2\pi R T_{\text{tr}-})^{3/2} (R T_{\text{int}-})^{\delta_-/2} \Gamma(\delta_-/2)} \exp \left(-\frac{(\xi_1 - v_-)^2 + \xi_2^2 + \xi_3^2}{2 R T_{\text{tr}-}} - \frac{\mathscr{E}}{R T_{\text{int}-}} \right), \quad (X_1 \to -\infty), \tag{110a}$$

$$f = \frac{\rho_+ \mathscr{E}^{\delta_+/2-1}}{(2\pi R T_{\text{tr}+})^{3/2} (R T_{\text{int}+})^{\delta_+/2} \Gamma(\delta_+/2)} \exp \left(-\frac{(\xi_1 - v_+)^2 + \xi_2^2 + \xi_3^2}{2 R T_{\text{tr}+}} - \frac{\mathscr{E}}{R T_{\text{int}+}} \right), \quad (X_1 \to \infty), \tag{110b}$$

where δ_- and δ_+ are, respectively, determined by the following equations:

$$\delta_- = D(T_-), \qquad T_- = E^{-1}(3RT_{\text{tr}-}/2 + \delta_- R T_{\text{int}-}/2), \tag{111a}$$

$$\delta_+ = D(T_+), \qquad T_+ = E^{-1}(3RT_{\text{tr}+}/2 + \delta_+ R T_{\text{int}+}/2). \tag{111b}$$

The existence and uniqueness of the solution (T_-, δ_-) or (T_+, δ_+) are discussed in the proof of Proposition 2′.

Applying (108) between the upstream and downstream equilibrium states and noting that $\boldsymbol{v}_\pm = (v_\pm, 0, 0)$, $(p_{ij})_\pm = R\rho_\pm T_{\text{tr}\pm} \delta_{ij}$, $(q_{\text{tr}})_{i\pm} = (q_{\text{int}})_{i\pm} = 0$, $e_{\text{tr}\pm} = 3RT_{\text{tr}\pm}/2$, and $e_{\text{int}\pm} = \delta_\pm R T_{\text{int}\pm}/2$, we obtain the following relations:

$$\rho_- v_- = \rho_+ v_+, \tag{112a}$$

$$R\rho_- T_{\text{tr}-} + \rho_- v_-^2 = R\rho_+ T_{\text{tr}+} + \rho_+ v_+^2, \tag{112b}$$

$$\rho_- v_- \left(\frac{5}{2} R T_{\text{tr}-} + \frac{1}{2} v_-^2 \right) = \rho_+ v_+ \left(\frac{5}{2} R T_{\text{tr}+} + \frac{1}{2} v_+^2 \right), \tag{112c}$$

$$\rho_- v_- \frac{\delta_-}{2} R T_{\text{int}-} = \rho_+ v_+ \frac{\delta_+}{2} R T_{\text{int}+}. \tag{112d}$$

From (112a) and (112d), we readily obtain

$$\delta_- T_{\text{int}-} = \delta_+ T_{\text{int}+}. \tag{113}$$

Here, we should note that (112a)–(112c) give the relations exactly the same as the Rankine–Hugoniot relations for a monatomic gas if we define the upstream Mach number based on $T_{\text{tr}-}$, that is,

$$\frac{\rho_+}{\rho_-} = \frac{4\widetilde{M}_-^2}{\widetilde{M}_-^2 + 3}, \qquad \frac{v_+}{v_-} = \frac{\widetilde{M}_-^2 + 3}{4\widetilde{M}_-^2}, \qquad \frac{T_{\mathrm{tr}+}}{T_{\mathrm{tr}-}} = \frac{(5\widetilde{M}_-^2 - 1)(\widetilde{M}_-^2 + 3)}{16\widetilde{M}_-^2}, \tag{114a}$$

$$\widetilde{M}_- = \frac{v_-}{\sqrt{5RT_{\mathrm{tr}-}/3}} = M_- \sqrt{\frac{3\gamma_-}{5(T_{\mathrm{tr}-}/T_-)}}. \tag{114b}$$

If we define $d_E(T) = E(T) - E(T_-)$ as in Appendix B.1, we have

$$d_E(T_+) = E(T_+) - E(T_-) = \frac{3}{2} R\left(T_{\mathrm{tr}+} - T_{\mathrm{tr}-}\right). \tag{115}$$

Using symbols $\tau = T_+/T_-$ and $\hat{d}_E$ [cf. (94a)] appeared in Appendix B.1, we obtain the relation

$$\hat{d}_E(\tau) = \frac{3}{2}\left(\frac{T_{\mathrm{tr}+}}{T_{\mathrm{tr}-}} - 1\right)\frac{T_{\mathrm{tr}-}}{T_-} = \frac{3}{2}\frac{(5\widetilde{M}_-^2 + 3)(\widetilde{M}_-^2 - 1)}{16\widetilde{M}_-^2}\frac{T_{\mathrm{tr}-}}{T_-}, \tag{116}$$

which determines τ, i.e., T_+. In addition, the following relations hold, as explained below:

$$\frac{T_{\mathrm{int}+}}{T_{\mathrm{int}-}} = \frac{\delta_-}{\delta_+}, \qquad \delta_+ = \frac{1}{\tau}\left[3 + \delta_- + 2\hat{d}_E(\tau)\right] - 3, \tag{117}$$

and δ_+ and $T_{\mathrm{int}+}$ are determined by these relations. The first equation of (117) is the direct consequence of (113). On the other hand, it follows from (111b), (4), and (115) that $\delta_+ = D(T_+) = (2/RT_+)E(T_+) - 3 = (2/RT_+)[d_E(T_+) + E(T_-)] - 3$. From (111a) and (11), we know that $E(T_-) = 3RT_{\mathrm{tr}-}/2 + \delta_- RT_{\mathrm{int}-}/2 = (3 + \delta_-)RT_-/2$. Combining these two relations and using the definition of $\hat{d}_E$, we obtain the second equation of (117).

The relations obtained above give the Rankine–Hugoniot relations for $\theta = 0$, which is summarized as follows:

Proposition 5′ (Rankine–Hugoniot relations for $\theta = 0$): For given upstream parameters ρ_-, v_-, $T_{\mathrm{tr}-}$, and $T_{\mathrm{int}-}$, the additional upstream parameters T_- and δ_- are determined by (111a). Then, the downstream parameters ρ_+, v_+, and $T_{\mathrm{tr}+}$ are determined by (114). In addition, the additional downstream parameters T_+, $T_{\mathrm{int}+}$, and δ_+ are determined by (116) and (117).

C Derivation of the macroscopic equations

In this appendix, we consider the case of large ratio μ_b/μ (or small θ) and obtain the slowly varying solution of (36) whose length scale of variation is of the order of $1/\theta$. Although the concept of the slowly varying solution appeared in connection with the problem of shock-wave structure, which is spatially one dimensional, we consider the more general spatially three-dimensional case where $f = f(X_i, \xi_i, \mathscr{E})$. Then, we need to extend the dimensionless equation (36) to the three-dimensional case with $\hat{f} = \hat{f}(x_i, \zeta_i, \hat{\mathscr{E}})$, i.e.,

$$\zeta_i \frac{\partial \hat{f}}{\partial x_i} = \frac{2}{\sqrt{\pi}} \hat{Q}(\hat{f}). \tag{118}$$

In this case, the parameters ρ_-, T_-, and p_- in (35) should be interpreted as the reference density, temperature, and pressure, and the flow velocity $\boldsymbol{v}$ or $\hat{\boldsymbol{v}}$ has the three components, $\boldsymbol{v} = (v_1, v_2, v_3)$ or $\hat{\boldsymbol{v}} = (\hat{v}_1, \hat{v}_2, \hat{v}_3)$. Then, (37)–(42) are valid as they stand.

The analysis here is in parallel to that in Appendix C in [27]. The only difference is that the internal degrees of freedom δ is constant in [27] but is a function of the temperature $\hat{T}$ here. Therefore, we avoid repeating the same equations quoting [27] occasionally and emphasize the different points.

C.1 Hilbert expansion

If we introduce a new space coordinates $y_i = (2/\sqrt{\pi})\theta x_i$ [cf. (63)] whose length scale of variation is of $O(1/\theta)$, then, (118) becomes

$$\theta \zeta_i \frac{\partial \hat{f}}{\partial y_i} = \hat{A}_c(\hat{T})\hat{\rho}(\hat{\mathscr{G}} - \hat{f}). \tag{119}$$

With the assumption that $\theta \ll 1$, we expand $\hat{f}$ as a power series in θ:

$$\hat{f} = \hat{f}^{(0)} + \hat{f}^{(1)}\theta + \hat{f}^{(2)}\theta^2 + \cdots. \tag{120}$$

Correspondingly, the macroscopic quantities $\hat{\rho}$, $\hat{v}_i$, $\hat{p}_{ij}$, ..., which are represented by $\hat{h}$, are also expanded as

$$\hat{h} = \hat{h}^{(0)} + \hat{h}^{(1)}\theta + \hat{h}^{(2)}\theta^2 + \cdots. \tag{121}$$

The expansions of $\hat{\rho}$, $\hat{v}_i$, $\hat{p}_{ij}$, $\hat{e}_{\mathrm{tr}}$, $\hat{e}_{\mathrm{int}}$, and thus $\hat{e}$ follow straightforwardly from (38c), (38d), and (39). The expressions of the expansion coefficients $\hat{\rho}^{(k)}$ ($k = 0, 1, 2, \ldots$), $\hat{v}_i^{(0)}$, $\hat{v}_i^{(1)}$, $\hat{p}_{ij}^{(0)}$, and $\hat{p}_{ij}^{(1)}$ in terms of $\hat{f}^{(l)}$ ($l = 0, 1, \ldots$) are given by (C5), (C6), and (C7) in [27], and the expressions of $\hat{e}^{(k)}$, $\hat{e}_{\mathrm{tr}}^{(k)}$, and $\hat{e}_{\mathrm{int}}^{(k)}$ ($k = 0, 1$) are given as

$$\hat{e}^{(k)} = \hat{e}_{\mathrm{tr}}^{(k)} + \hat{e}_{\mathrm{int}}^{(k)}, \qquad (k = 0, 1), \tag{122}$$

$$\hat{e}_{\mathrm{tr}}^{(0)} = \frac{1}{\hat{\rho}^{(0)}} \iint_0^\infty |\boldsymbol{\zeta} - \hat{\boldsymbol{v}}^{(0)}|^2 \hat{f}^{(0)} d\hat{\mathscr{E}} d\boldsymbol{\zeta}, \tag{123a}$$

$$\hat{e}_{\mathrm{tr}}^{(1)} = \frac{1}{\hat{\rho}^{(0)}} \iint_0^\infty |\boldsymbol{\zeta} - \hat{\boldsymbol{v}}^{(0)}|^2 \hat{f}^{(1)} d\hat{\mathscr{E}} d\boldsymbol{\zeta} - \frac{\hat{\rho}^{(1)}}{\hat{\rho}^{(0)}} \hat{e}_{\mathrm{tr}}^{(0)}, \tag{123b}$$

$$\hat{e}_{\mathrm{int}}^{(0)} = \frac{1}{\hat{\rho}^{(0)}} \iint_0^\infty \hat{\mathscr{E}} \hat{f}^{(0)} d\hat{\mathscr{E}} d\boldsymbol{\zeta}, \tag{124a}$$

$$\hat{e}_{\mathrm{int}}^{(1)} = \frac{1}{\hat{\rho}^{(0)}} \iint_0^\infty \hat{\mathscr{E}} \hat{f}^{(1)} d\hat{\mathscr{E}} d\boldsymbol{\zeta} - \frac{\hat{\rho}^{(1)}}{\hat{\rho}^{(0)}} \hat{e}_{\mathrm{int}}^{(0)}. \tag{124b}$$

With the expansion of $\hat{e}$, (38e) leads to the expansion of $\hat{T}$ and thus that of δ. To be more specific, their expansion coefficients are obtained as

$$\hat{T}^{(0)} = \hat{E}^{-1}(\hat{e}^{(0)}), \qquad \hat{T}^{(1)} = \left(\frac{d\hat{E}}{d\hat{T}}\right)^{-1}_{\hat{T}=\hat{T}^{(0)}} \hat{e}^{(1)}, \tag{125a}$$

$$\delta^{(0)} = \hat{D}(\hat{T}^{(0)}), \qquad \delta^{(1)} = \left(\frac{d\hat{D}}{d\hat{T}}\right)_{\hat{T}=\hat{T}^{(0)}} \hat{T}^{(1)}. \tag{125b}$$

Then, the expansions of $\hat{T}_{\mathrm{tr}}$, $\hat{T}_{\mathrm{int}}$, and $\hat{T}_{\mathrm{rel}}$ follow from (38f). That is, their expansion coefficients are obtained as

$$\hat{T}_{\mathrm{tr}}^{(0)} = (2/3)\hat{e}_{\mathrm{tr}}^{(0)}, \qquad \hat{T}_{\mathrm{tr}}^{(1)} = (2/3)\hat{e}_{\mathrm{tr}}^{(1)}, \tag{126a}$$

$$\hat{T}_{\mathrm{int}}^{(0)} = 2\hat{e}_{\mathrm{int}}^{(0)}/\delta^{(0)}, \qquad \hat{T}_{\mathrm{int}}^{(1)} = (2/\delta^{(0)})[\hat{e}_{\mathrm{int}}^{(1)} - (\delta^{(1)}/\delta^{(0)})\hat{e}_{\mathrm{int}}^{(0)}], \tag{126b}$$

$$\hat{T}_{\mathrm{rel}}^{(0)} = \hat{T}_{\mathrm{int}}^{(0)}, \qquad \hat{T}_{\mathrm{rel}}^{(1)} = \hat{T}_{\mathrm{int}}^{(1)} + \hat{T}^{(0)} - \hat{T}_{\mathrm{int}}^{(0)}. \tag{126c}$$

In consequence, $\hat{A}_c(\hat{T})$ and $\hat{\mathscr{G}}$ are also expanded in θ. The expansion of $\hat{A}_c(\hat{T})$ is the same as (C12a), (C13a), and (C13b) in [27], that is, the expansion coefficients $\hat{A}_c^{(0)}$ and $\hat{A}_c^{(1)}$ are given as

$$\hat{A}_c^{(0)} = \hat{A}_c(\hat{T}^{(0)}), \qquad \hat{A}_c^{(1)} = \left(\frac{d\hat{A}_c}{d\hat{T}}\right)_{\hat{T}=\hat{T}^{(0)}} \hat{T}^{(1)}. \tag{127}$$

On the other hand, the expansion of $\hat{\mathscr{G}}$, which is in the form of (C12b) in [27], has slightly different expansion coefficients from (C13c), (C13d), and (C14) in [27]. That is, the coefficients $\hat{\mathscr{G}}^{(0)}$ and $\hat{\mathscr{G}}^{(1)}$ are obtained as follows:

$$\hat{\mathscr{G}}^{(0)} = \frac{\hat{\rho}^{(0)}\hat{\mathscr{E}}^{\delta^{(0)}/2-1}}{\pi^{3/2}([\det(\hat{\mathsf{T}})]^{(0)})^{1/2}(\hat{T}_{\mathrm{rel}}^{(0)})^{\delta^{(0)}/2}\Gamma(\delta^{(0)}/2)} \times \exp\left(-(\hat{\mathsf{T}}^{-1})_{ij}^{(0)}(\zeta_i - \hat{v}_i^{(0)})(\zeta_j - \hat{v}_j^{(0)}) - \frac{\hat{\mathscr{E}}}{\hat{T}_{\mathrm{rel}}^{(0)}}\right), \tag{128a}$$

$$\hat{\mathscr{G}}^{(1)} = \hat{\mathscr{G}}^{(0)}\Psi^{(1)}, \tag{128b}$$

where

$$\Psi^{(1)} = \frac{\delta^{(1)}}{2}\left[\ln\frac{\hat{\mathscr{E}}}{\hat{T}_{\mathrm{rel}}^{(0)}} - \frac{\Gamma'(\delta^{(0)}/2)}{\Gamma(\delta^{(0)}/2)}\right] + \frac{\hat{\rho}^{(1)}}{\hat{\rho}^{(0)}} - \frac{1}{2}\frac{[\det(\hat{\mathsf{T}})]^{(1)}}{[\det(\hat{\mathsf{T}})]^{(0)}} + \frac{\hat{T}_{\mathrm{rel}}^{(1)}}{\hat{T}_{\mathrm{rel}}^{(0)}}\left(\frac{\hat{\mathscr{E}}}{\hat{T}_{\mathrm{rel}}^{(0)}} - \frac{\delta^{(0)}}{2}\right) - (\hat{\mathsf{T}}^{-1})_{ij}^{(1)}(\zeta_i - \hat{v}_i^{(0)})(\zeta_j - \hat{v}_j^{(0)}) + (\hat{\mathsf{T}}^{-1})_{ij}^{(0)}\hat{v}_i^{(1)}(\zeta_j - \hat{v}_j^{(0)}) + (\hat{\mathsf{T}}^{-1})_{ij}^{(0)}(\zeta_i - \hat{v}_i^{(0)})\hat{v}_j^{(1)}. \tag{129}$$

Here, $\hat{\mathsf{T}}^{(k)}$, $(\hat{\mathsf{T}}^{-1})^{(k)}$, and $[\det(\hat{\mathsf{T}})]^{(k)}$ ($k = 0$ and 1) are the coefficients of the expansions of $\hat{\mathsf{T}}$, $\hat{\mathsf{T}}^{-1}$, and $\det(\hat{\mathsf{T}})$ in the form of (C15) in [27] and are given by (C19), (C21), and (C22) in [27].

With these preparations, we can proceed with the procedure following Appendix C in [27]. The integral equations for the expansion coefficients $\hat{f}^{(0)}$ and $\hat{f}^{(1)}$ [cf. (120)] are readily obtained in the form of (C23) and (C25) in [27], i.e.,

$$\hat{f}^{(0)} = \hat{\mathscr{G}}^{(0)}, \tag{130a}$$

$$\hat{f}^{(1)} = \hat{\mathscr{G}}^{(1)} - \frac{1}{\hat{A}_c^{(0)}\hat{\rho}^{(0)}}\zeta_i\frac{\partial \hat{f}^{(0)}}{\partial y_i}, \tag{130b}$$

with the constraint

$$\iint_0^\infty \begin{pmatrix} \zeta_j \\ \zeta_i\zeta_j \\ (\zeta_k^2 + \hat{\mathscr{E}})\zeta_j \end{pmatrix} \frac{\partial \hat{f}^{(0)}}{\partial y_j} d\hat{\mathscr{E}} d\boldsymbol{\zeta} = 0, \tag{131}$$

for (130b).

The solution of (130a) is obtained in the following form:

$$\hat{f}^{(0)} = \frac{\hat{\rho}^{(0)}\hat{\mathscr{E}}^{\delta^{(0)}/2-1}}{(\pi\hat{T}_{\mathrm{tr}}^{(0)})^{3/2}(\hat{T}_{\mathrm{int}}^{(0)})^{\delta^{(0)}/2}\Gamma(\delta^{(0)}/2)}\exp\left(-\frac{(\zeta_k - \hat{v}_k^{(0)})^2}{\hat{T}_{\mathrm{tr}}^{(0)}} - \frac{\hat{\mathscr{E}}}{\hat{T}_{\mathrm{int}}^{(0)}}\right), \tag{132}$$

where $\delta^{(0)}$ is related to $\hat{T}_{\mathrm{tr}}^{(0)}$ and $\hat{T}_{\mathrm{int}}^{(0)}$ by the relations

$$\delta^{(0)} = \hat{D}(\hat{T}^{(0)}), \qquad \hat{T}^{(0)} = \hat{E}^{-1}(3\hat{T}_{\mathrm{tr}}^{(0)}/2 + \delta^{(0)}\hat{T}_{\mathrm{int}}^{(0)}/2). \tag{133}$$

These relations are obtained from (122), (125), (126a), and (126b). In (132), $\hat{\rho}^{(0)}$, $\hat{v}_i^{(0)}$, $\hat{T}_{\mathrm{tr}}^{(0)}$, and $\hat{T}_{\mathrm{int}}^{(0)}$ are unknown functions, and their equations are shown later. It is seen from (81) and (82) that $\hat{f}^{(0)}$ is the dimensionless form of a local equilibrium distribution for $\theta = 0$. This $\hat{f}^{(0)}$ is of the same form as $\hat{f}^{(0)}$ in [27] [(C30) there] except that the constant δ is replaced with the function $\delta^{(0)}$.

From (130) and after some algebra, the first-order solution $\hat{f}^{(1)}$ can be expressed in the following form [cf. (C31) and (C33) in [27]]:

$$\hat{f}^{(1)} = \hat{f}^{(0)}\Psi^{(1)} - \frac{1}{\hat{A}_c^{(0)}\hat{\rho}^{(0)}}\zeta_i \frac{\partial \hat{f}^{(0)}}{\partial y_i}, \tag{134}$$

where

$$\begin{aligned}\Psi^{(1)} = {} & \frac{\delta^{(1)}}{2}\left[\ln\frac{\hat{\mathscr{E}}}{\hat{T}_{\rm int}^{(0)}} - \frac{\Gamma'(\delta^{(0)}/2)}{\Gamma(\delta^{(0)}/2)}\right] + \frac{\hat{\rho}^{(1)}}{\hat{\rho}^{(0)}} + 2\frac{(\zeta_j - \hat{v}_j^{(0)})\hat{v}_j^{(1)}}{\hat{T}_{\rm tr}^{(0)}} \\ & + \frac{1}{\hat{T}_{\rm tr}^{(0)}}\left[\hat{T}_{\rm tr}^{(1)} + \left(\hat{T}^{(0)} - \hat{T}_{\rm tr}^{(0)}\right)\right]\left[\frac{(\zeta_k - \hat{v}_k^{(0)})^2}{\hat{T}_{\rm tr}^{(0)}} - \frac{3}{2}\right] \\ & + \frac{1}{\hat{T}_{\rm int}^{(0)}}\left[\hat{T}_{\rm int}^{(1)} + \left(\hat{T}^{(0)} - \hat{T}_{\rm int}^{(0)}\right)\right]\left(\frac{\hat{\mathscr{E}}}{\hat{T}_{\rm int}^{(0)}} - \frac{\delta^{(0)}}{2}\right) \\ & + \nu\frac{1}{\hat{\rho}^{(0)}\hat{T}_{\rm tr}^{(0)}}\left(\hat{p}_{ij}^{(1)} - \frac{1}{3}\hat{p}_{kk}^{(1)}\delta_{ij}\right)\frac{(\zeta_i - \hat{v}_i^{(0)})(\zeta_j - \hat{v}_j^{(0)})}{\hat{T}_{\rm tr}^{(0)}}.\end{aligned} \tag{135}$$

The solution $\hat{f}^{(1)}$, given by (134) with (132) and (135), is of the same form as $\hat{f}^{(1)}$ in [27] [cf. (C31) with (C30) and (C33) there], except that the new term $(\delta^{(1)}/2)\,[\,\ln(\hat{\mathscr{E}}/\hat{T}_{\rm int}^{(0)}) - \Gamma'(\delta^{(0)}/2)/\Gamma(\delta^{(0)}/2)\,]$ appears and the constant δ is replaced with the function $\delta^{(0)}$ in (135). It is noted that in connection with the new term, the following relation holds:

$$\int_0^\infty \left[\ln\frac{\hat{\mathscr{E}}}{\hat{T}_{\rm int}^{(0)}} - \frac{\Gamma'(\delta^{(0)}/2)}{\Gamma(\delta^{(0)}/2)}\right]\hat{f}^{(0)} d\mathscr{E} = 0. \tag{136}$$

C.2 Macroscopic equations

Substituting (132) into (131), we obtain the following equations containing six functions $\hat{\rho}^{(0)}$, $\hat{v}_j^{(0)}$, $\hat{T}_{\rm tr}^{(0)}$, and $\hat{T}_{\rm int}^{(0)}$ [cf. (C34) in [27]]:

$$\frac{\partial}{\partial y_j}\left(\hat{\rho}^{(0)}\hat{v}_j^{(0)}\right) = 0, \tag{137a}$$

$$\frac{\partial}{\partial y_j}\left(\frac{1}{2}\hat{\rho}^{(0)}\hat{T}_{\rm tr}^{(0)}\delta_{ij} + \hat{\rho}^{(0)}\hat{v}_i^{(0)}\hat{v}_j^{(0)}\right) = 0, \tag{137b}$$

$$\frac{\partial}{\partial y_j}\left[\hat{\rho}^{(0)}\hat{v}_j^{(0)}(\hat{v}_k^{(0)})^2 + \hat{\rho}^{(0)}\hat{v}_j^{(0)}\frac{5\hat{T}_{\rm tr}^{(0)} + \delta^{(0)}\hat{T}_{\rm int}^{(0)}}{2}\right] = 0. \tag{137c}$$

By appropriate combination, these equations can also be transformed into the following form:

$$\frac{\partial}{\partial y_j}\left(\hat{\rho}^{(0)}\hat{v}_j^{(0)}\right) = 0, \tag{138a}$$

$$\hat{\rho}^{(0)}\hat{v}_j^{(0)}\frac{\partial \hat{v}_i^{(0)}}{\partial y_j} + \frac{1}{2}\frac{\partial}{\partial y_i}\left(\hat{\rho}^{(0)}\hat{T}_{\rm tr}^{(0)}\right) = 0, \tag{138b}$$

$$\hat{v}_j^{(0)}\frac{\partial}{\partial y_j}\left(3\hat{T}_{\rm tr}^{(0)} + \delta^{(0)}\hat{T}_{\rm int}^{(0)}\right) + 2\hat{T}_{\rm tr}^{(0)}\frac{\partial \hat{v}_j^{(0)}}{\partial y_j} = 0, \tag{138c}$$

where we have made use of (138b) multiplied by $\hat{v}_i^{(0)}$ in deriving (138c). It should be noted here that $\delta^{(0)}$ is a function of $\hat{T}_{\rm tr}^{(0)}$ and $\hat{T}_{\rm int}^{(0)}$ defined implicitly by (133). Therefore, we need one more equation to close the system.

As in [27], we calculate the first-order quantities $\hat{\rho}^{(1)}$, $\hat{v}_i^{(1)}$, $\hat{p}_{ij}^{(1)}$, $\hat{T}_{\rm tr}^{(1)}$, and $\hat{T}_{\rm int}^{(1)}$ using their definitions and (134). Because of the relation (136), these calculations of $\hat{\rho}^{(1)}$, $\hat{v}_i^{(1)}$, $\hat{p}_{ij}^{(1)}$, and $\hat{T}_{\rm tr}^{(1)}$ are basically the same as those in [27]. More specifically, the calculation for $\hat{\rho}^{(1)}$ and $\hat{v}_i^{(1)}$ gives trivial (or consistent) result, i.e., $\hat{\rho}^{(1)} = \hat{\rho}^{(1)}$ and $\hat{v}_i^{(1)} = \hat{v}_i^{(1)}$, and that for $\hat{p}_{ij}^{(1)}$ gives the following expression of $\hat{p}_{ij}^{(1)}$:

$$\begin{aligned}\hat{p}_{ij}^{(1)} &= (\hat{\rho}^{(0)}\hat{T}_{\rm tr}^{(1)} + \hat{\rho}^{(1)}\hat{T}_{\rm tr}^{(0)})\delta_{ij} + \frac{1}{1-\nu}\hat{\rho}^{(0)}\left(\hat{T}^{(0)} - \hat{T}_{\rm tr}^{(0)}\right)\delta_{ij} \\ &\quad - \frac{1}{1-\nu}\frac{\hat{T}_{\rm tr}^{(0)}}{\hat{A}_c^{(0)}}\left(\frac{\partial \hat{v}_i^{(0)}}{\partial y_j} + \frac{\partial \hat{v}_j^{(0)}}{\partial y_i} + \frac{\partial \hat{v}_k^{(0)}}{\partial y_k}\delta_{ij}\right) \\ &\quad - \frac{1}{1-\nu}\frac{\hat{v}_k^{(0)}}{\hat{A}_c^{(0)}\hat{\rho}^{(0)}}\frac{\partial}{\partial y_k}\left(\hat{\rho}^{(0)}\hat{T}_{\rm tr}^{(0)}\right)\delta_{ij}. \end{aligned} \tag{139}$$

The calculation of $\hat{T}_{\rm tr}^{(1)}$ using (123b) and (126a), or equivalently $\hat{\rho}^{(0)}\hat{T}_{\rm tr}^{(1)} + \hat{\rho}^{(1)}\hat{T}_{\rm tr}^{(0)} = (1/3)\hat{p}_{kk}^{(1)}$, and (137a) lead to the following relation:

$$\hat{v}_k^{(0)}\frac{\partial \hat{T}_{\rm tr}^{(0)}}{\partial y_k} = \hat{A}_c^{(0)}\hat{\rho}^{(0)}\left(\hat{T}^{(0)} - \hat{T}_{\rm tr}^{(0)}\right) - \frac{2}{3}\hat{T}_{\rm tr}^{(0)}\frac{\partial \hat{v}_k^{(0)}}{\partial y_k}, \tag{140}$$

because the term $\hat{\rho}^{(0)}\hat{T}_{\rm tr}^{(1)} + \hat{\rho}^{(1)}\hat{T}_{\rm tr}^{(0)}$ is canceled out. On the other hands, the calculation of $\hat{T}_{\rm int}^{(1)}$ is slightly different from that in [27] because of the presence of the term containing $\delta^{(1)}$ in (126b). If we calculate $\hat{T}_{\rm int}^{(1)}$ using (124b) and (126b), or equivalently

$$\begin{aligned}&\hat{\rho}^{(0)}\hat{T}_{\rm int}^{(1)} + \hat{\rho}^{(1)}\hat{T}_{\rm int}^{(0)} + \frac{\delta^{(1)}}{\delta^{(0)}}\hat{\rho}^{(0)}\hat{T}_{\rm int}^{(0)} \\ &\quad = \frac{2}{\delta^{(0)}}\iint_0^\infty \hat{\mathscr{E}}\hat{f}^{(1)}d\hat{\mathscr{E}}d\boldsymbol{\zeta} \\ &\quad = \frac{2}{\delta^{(0)}}\iint_0^\infty \hat{\mathscr{E}}\left(\hat{f}^{(0)}\Psi^{(1)} - \frac{1}{\hat{A}_c^{(0)}\hat{\rho}^{(0)}}\zeta_k\frac{\partial \hat{f}^{(0)}}{\partial y_k}\right)d\hat{\mathscr{E}}d\boldsymbol{\zeta}, \end{aligned} \tag{141}$$

then the term $\hat{\rho}^{(0)}\hat{T}_{\rm int}^{(1)} + \hat{\rho}^{(1)}\hat{T}_{\rm int}^{(0)} + (\delta^{(1)}/\delta^{(0)})\hat{\rho}^{(0)}\hat{T}_{\rm int}^{(0)}$ is canceled out, and we obtain

$$\hat{v}_k^{(0)}\frac{\partial(\delta^{(0)}\hat{T}_{\rm int}^{(0)})}{\partial y_k} = \hat{A}_c^{(0)}\delta^{(0)}\hat{\rho}^{(0)}\left(\hat{T}^{(0)} - \hat{T}_{\rm int}^{(0)}\right), \tag{142}$$

where use has been made of (137a). Here we should note that $\hat{A}_c^{(0)}$ and $\delta^{(0)}$ are the known functions of $\hat{T}^{(0)}$, which is expressed in terms of $\hat{T}_{\rm tr}^{(0)}$ and $\hat{T}_{\rm int}^{(0)}$ by (133). Therefore, (140) and (142) contain only $\hat{\rho}^{(0)}$, $\hat{v}_j^{(0)}$, $\hat{T}_{\rm tr}^{(0)}$, and $\hat{T}_{\rm int}^{(0)}$. This means that either (140) or (142) can be the additional equation to make the system (137) closed. In fact, we can choose one of them because (140) and (142) are not independent. More specifically, if we add (140) multiplied by 3 and (142) and take into account the relation

$$(3 + \delta^{(0)})\hat{T}^{(0)} = 3\hat{T}_{\rm tr}^{(0)} + \delta^{(0)}\hat{T}_{\rm int}^{(0)}, \tag{143}$$

which follows from (40b) and (133), then we obtain (138c).

In summary, the macroscopic system for $\hat{\rho}^{(0)}$, $\hat{v}_j^{(0)}$, $\hat{T}_{\mathrm{tr}}^{(0)}$, and $\hat{T}_{\mathrm{int}}^{(0)}$, which corresponds to the slowly varying solution, is provided by (137) [or (138)] and (140) or (142). In the calculation for the structure of a shock wave in CO_2 gas in Sect. 3.7, we use (137) and (142).

In concluding this appendix, we give a brief remark on the ET6 system that has been used in the calculation of shock-wave structure in [53,40,54]. The linear ET6 system is a hyperbolic system for the 6 macroscopic variables, the density ρ, flow velocity v_i, pressure p, and dynamic pressure Π, valid for a general polyatomic gas with temperature-dependent specific heats but for small deviation from a local equilibrium state. It was derived macroscopically by the phenomenological theory of extended thermodynamics in [6], and its version for a gas with constant specific heats has been derived from kinetic theory with appropriate closure assumptions [6,44]. It has also been extended to the case where the deviation from the equilibrium state is large in [5] (the nonlinear ET6 system), which is the same as the linear ET6 system except that the nonlinearity appears in the source term in the equation for Π. More recently, the ET6 system has been derived from kinetic theory in a more general setting, which allows the temperature-dependent specific heats, by suitable closure assumptions [9].

Let us consider the ET6 system presented by (49) in [9] and adopt the BGK source term, (113) in [9]. The comparison in the level of kinetic theory shows that Π and ε there are, respectively, equivalent to $p_{kk}/3 - p = R\rho(T_{\mathrm{tr}} - T)$ and $E(T)$ in the present paper. We further note that $E(T) = (3+\delta)RT/2$ and $T = (3T_{\mathrm{tr}} + \delta T_{\mathrm{int}})/(3+\delta)$, where $\delta = D(T)$, and use these relations in the steady version ($\partial/\partial t = 0$) of (49) with (113) in [9]. Then, the first to the third equations are transformed to the dimensional versions of (137a), (137b), and (137c), respectively, and the fourth equation is reduced to

$$v_i \frac{\partial \delta T_{\mathrm{int}}}{\partial X_i} = \frac{\delta}{\tau}(T - T_{\mathrm{int}}), \tag{144}$$

where τ is the BGK relaxation time, and X_i is used for the dimensional space coordinates in accordance with the notation in the present paper. If we let $\tau = 1/\theta\rho A_c(T)$, the dimensionless version of (144) is found to be the same as (142). In summary, the macroscopic equations (137) and (142) for small θ are essentially the same as the steady version of the ET6 system. Since it is just a straightforward matter to include the time-derivative terms in (137) and (142), the present asymptotic analysis for small θ (or large relaxation time) provides an alternative way to derive the ET6 system from kinetic theory without any closure assumptions.

D Stability analysis for (72)

In this appendix, we discuss the local stability of the equilibrium solutions of (72). We first consider the equilibrium point $\hat{v}_1 = \hat{v}_-$ and then $\hat{v}_1 = \hat{v}_+$.

Let us rewrite (72a) in the following form:

$$\frac{d\hat{v}_1}{dy_1} = F(\hat{v}_1), \tag{145}$$

where

$$F(\hat{v}_1) = G(\hat{v}_1)P(\hat{v}_1), \quad G(\hat{v}_1) = \frac{3\hat{v}_-}{8}\frac{\hat{A}_c(\hat{T})}{\hat{v}_1^2(\hat{v}_* - \hat{v}_1)}, \quad P(\hat{v}_1) = \hat{v}_1^2 - \frac{1+2\hat{v}_-^2}{2\hat{v}_-}\hat{v}_1 + \frac{1}{2}\hat{T}, \tag{146}$$

and $\hat{v}_*$ is given by (73). In addition, since $\hat{E}(\hat{T}) = (3+\delta)\hat{T}/2$, (72c) can be rewritten as

$$\hat{T} = \hat{E}^{-1}(\hat{e}), \qquad \hat{e} = \frac{3+\delta_-}{2} + (\hat{v}_1 - \hat{v}_-)\left(\hat{v}_1 - \frac{1+\hat{v}_-^2}{\hat{v}_-}\right). \tag{147}$$

Let us investigate the behavior of $F(\hat{v}_1)$ near $\hat{v}_1 = \hat{v}_-$. Since $P(\hat{v}_-) = 0$, $F(\hat{v}_1)$ is Taylor expended around $\hat{v}_1 = \hat{v}_-$ as

$$F(\hat{v}_1) = G(\hat{v}_-)\left(\frac{dP}{d\hat{v}_1}\right)_{\hat{v}_1=\hat{v}_-}(\hat{v}_1 - \hat{v}_-) + O(|\hat{v}_1 - \hat{v}_-|^2). \tag{148}$$

Noting that $d\hat{E}(\hat{T})/d\hat{T} = \hat{C}_v(\hat{T})$ [cf. (40a)], we obtain, from (146) and (147), that

$$\frac{dP(\hat{v}_1)}{d\hat{v}_1} = 2\hat{v}_1 - \frac{1+2\hat{v}_-^2}{2\hat{v}_-} + \frac{1}{\hat{C}_v(\hat{T})}\left(\hat{v}_1 - \frac{1+2\hat{v}_-^2}{2\hat{v}_-}\right), \tag{149}$$

which leads to $(dP/d\hat{v}_1)_{\hat{v}_1=\hat{v}_-} = \hat{v}_- - (\gamma_-/2\hat{v}_-)$, where use has been made of the fact that $\hat{T} = 1$ at $\hat{v}_1 = \hat{v}_-$ and $\gamma_- = 1 + R/C_v(T_-) = 1 + 1/\hat{C}_v(1)$ [cf. (30)]. Therefore, with the help of (73), (148) is transformed to the following expression:

$$\begin{aligned} F(\hat{v}_1) &= \frac{3\hat{A}_c(1)}{8\hat{v}_-}\frac{\hat{v}_- - (\gamma_-/2\hat{v}_-)}{\hat{v}_* - \hat{v}_-}(\hat{v}_1 - \hat{v}_-) + O(|\hat{v}_1 - \hat{v}_-|^2) \\ &= -\frac{\hat{A}_c(1)}{\hat{v}_-}\frac{\hat{v}_-^2 - (\gamma_-/2)}{\hat{v}_-^2 - (5/6)}(\hat{v}_1 - \hat{v}_-) + O(|\hat{v}_1 - \hat{v}_-|^2). \end{aligned} \tag{150}$$

In [27] for a gas with constant specific heats, it is shown that the slowly varying solution exhibits Type-A profile for $\widetilde{M}_- < 1 < M_-$, Type-B profile for $\widetilde{M}_- = 1 < M_-$, and Type-C profile for $1 < \widetilde{M}_- < M_-$ (see the last paragraph in Sect. 3.6.1 and [52]). Here, it should be noted that $\widetilde{M}_- = M_-\sqrt{3\gamma_-/5} < M_-$ holds from (114b) (with $T_{\mathrm{tr}-} = T_-$) and $\gamma_- < 5/3$. We observe (150) according to this classification assuming that $\hat{v}_1$ decreases monotonically from $\hat{v}_-$ to $\hat{v}_+$ as y_1 changes from $-\infty$ to ∞.

From (114b), it follows that $\hat{v}_- = \sqrt{5/6}\,\widetilde{M}_- = \sqrt{\gamma_-/2}\,M_-$. Therefore, we can see the following:

(i) For $\widetilde{M}_- < 1 < M_-$, the inequality $\sqrt{\gamma_-/2} < \hat{v}_- < \sqrt{5/6}$ holds, so that the coefficient of $\hat{v}_1 - \hat{v}_-$ in the second line in (150) is positive. This means that for any $\hat{v}_1 = \hat{v}_0\ (< \hat{v}_-)$ sufficiently close to $\hat{v}_-$, $F(\hat{v}_1)$ and thus $d\hat{v}_1/dy_1$ are negative. Therefore, as y_1 moves from its value corresponding to $\hat{v}_0$ to $-\infty$, $\hat{v}_1$ approaches $\hat{v}_-$. That is, $\hat{v}_-$ is a locally and asymptotically stable equilibrium point as y_1 tends to $-\infty$.

(ii) For $1 < \widetilde{M}_- (< M_-)$, the same coefficient of $\hat{v}_1 - \hat{v}_-$ in (150) is negative because $(\sqrt{\gamma_-/2} <)\sqrt{5/6} < \hat{v}_-$ holds. Therefore, since $d\hat{v}_1/dy_1$ is positive for any $\hat{v}_1 = \hat{v}_0\ (< \hat{v}_-)$ sufficiently close to $\hat{v}_-$, $\hat{v}_1$ does not converge to $\hat{v}_-$ as y_1 tends to $-\infty$. That is, $\hat{v}_-$ is an unstable equilibrium point as y_1 tends to $-\infty$.

(iii) For $\widetilde{M}_- = 1 (< M_-)$, it follows from (114b) and (73) that $\hat{v}_- = \hat{v}_* = \sqrt{5/6}$. In this case, $G(\hat{v}_1)$ is singular at $\hat{v}_1 = \hat{v}_-$. However, if we use the Taylor expansion of $P(\hat{v}_1)$ around $\hat{v}_1 = \hat{v}_-$ in $F(\hat{v}_1) = G(\hat{v}_1)P(\hat{v}_1)$, the factor $\hat{v}_1 - \hat{v}_*$ in the denominator of $G(\hat{v}_1)$ is canceled out, and we have the following expression of $F(\hat{v}_1)$:

$$F(\hat{v}_1) = -\frac{3\hat{v}_-}{8}\frac{\hat{A}_c(\hat{T})}{\hat{v}_1^2}\left[\frac{1}{2}\sqrt{\frac{6}{5}}\left(\frac{5}{3} - \gamma_-\right) + O(|\hat{v}_1 - \hat{v}_-|)\right]. \tag{151}$$

Since $F(\hat{v}_-) = -(9/40)\hat{A}_c(1)(5/3 - \gamma_-) < 0$ because of $\gamma_- < 5/3$, $\hat{v}_1 = \hat{v}_-$ is not an equilibrium point of (72) or (145).

Now we consider the behavior of $F(\hat{v}_1)$ near $\hat{v}_1 = \hat{v}_+$. With the help of the relations $1/\hat{v}_- + 2\hat{v}_- = \hat{T}_+/\hat{v}_+ + 2\hat{v}_+$ [cf. (70) and (71)] and $\gamma_+ = [C_v(T_+) + R]/C_v(T_+) = 1 + 1/\hat{C}_v(\hat{T}_+)$, (149) gives the following expression of $dP(\hat{v}_1)/d\hat{v}_1$ at $\hat{v}_1 = \hat{v}_+$:

$$\left(\frac{dP}{d\hat{v}_1}\right)_{\hat{v}_1=\hat{v}_+} = \hat{v}_+ - \frac{\gamma_+\hat{T}_+}{2\hat{v}_+}. \tag{152}$$

Since $P(\hat{v}_+) = 0$, $F(\hat{v}_1)$ is Taylor expanded around $\hat{v}_1 = \hat{v}_+$ as

$$\begin{aligned} F(\hat{v}_1) &= G(\hat{v}_+)\left(\frac{dP}{d\hat{v}_1}\right)_{\hat{v}_1=\hat{v}_+}(\hat{v}_1 - \hat{v}_+) + O(|\hat{v}_1 - \hat{v}_+|^2) \\ &= -\frac{\hat{v}_-\hat{A}_c(\hat{T}_+)}{\hat{v}_+^2}\frac{\hat{v}_+^2 - \gamma_+\hat{T}_+/2}{\hat{v}_+^2 - 5\hat{T}_+/6}(\hat{v}_1 - \hat{v}_+) + O(|\hat{v}_1 - \hat{v}_+|^2), \end{aligned} \tag{153}$$

where use has been made of the relation $\hat{v}_* = (5/16)(1/\hat{v}_- + 2\hat{v}_-) = (5/16)(\hat{T}_+/\hat{v}_+ + 2\hat{v}_+)$. Since the Mach number at downstream infinity $M_+ = v_+/(\gamma_+ RT_+)^{1/2} = (2/\gamma_+\hat{T}_+)^{1/2}\hat{v}_+$ is less than 1 [cf. the last paragraph in Sect. 3.1], we have $\hat{v}_+ < (\gamma_+\hat{T}_+/2)^{1/2} < (5\hat{T}_+/6)^{1/2}$ because of $\gamma_+ < 5/3$. Therefore, the coefficient of $\hat{v}_1 - \hat{v}_+$ in the second line in (153) is negative. This means that for any $\hat{v}_1 = \hat{v}_0$ ($> \hat{v}_+$) sufficiently close to $\hat{v}_+$, $F(\hat{v}_1)$ and thus $d\hat{v}_1/dy_1$ are negative. Therefore, as y_1 moves from its value corresponding to $\hat{v}_0$ to ∞, $\hat{v}_1$ approaches $\hat{v}_+$. That is, $\hat{v}_+$ is a locally and asymptotically stable equilibrium point as y_1 tends to ∞ for any M_-.

From the local stability and instability of the equilibrium points discussed above, we can conjecture the following behavior of the solution of (72):

(i) For $\widetilde{M}_- < 1 < M_-$, the solution provides a smooth and monotonically decreasing profile of $\hat{v}_1$ ranging from $\hat{v}_-$ to $\hat{v}_+$ as y_1 changes from $-\infty$ to ∞.

(ii) For $1 < \widetilde{M}_-(< M_-)$, although the profile of $\hat{v}_1$ approaches $\hat{v}_+$ as $y_1 \to \infty$, it cannot approach $\hat{v}_-$ as $y_1 \to -\infty$. Therefore, (72) should be solved from $y_1 = y_0$, where y_0 is a finite value, to $y_1 = \infty$, and the solution gives a partial profile of $\hat{v}_1$ for $y_0 \le y_1 < \infty$.

(iii) For $\widetilde{M}_- = 1(< M_-)$, $\hat{v}_1 = \hat{v}_-$ is not an equilibrium point of (72). Therefore, the solution does not approach $\hat{v}_-$ as $y_1 \to -\infty$. However, one may solve (72) under the initial condition that $\hat{v}_1 = \hat{v}_-$ at $y_1 = y_0$ with a finite y_0. Then, the solution exhibits the profile of $\hat{v}_1$ that starts suddenly from $\hat{v}_-$ at $y_1 = y_0$ and approaches $\hat{v}_+$ as $y_1 \to \infty$. Since $d\hat{v}_1/dy_1 < 0$ at $y_1 = y_0$, the profile has a corner there.

These properties of the slowly varying solution are essentially the same as that in the case of a gas with constant specific heats [27], and case (i) corresponds to Type-A profile, case (ii) corresponds to Type-C profile, and case (iii) corresponds to Type-B profile.

References

1. Alekseev, I.V., Kosareva, A.A., Kustova, E.V., Nagnibeda, E.A.: Various continuum approaches for studying shock wave structure in carbon dioxide. In: AIP Conference Proceedings The 8th Polyakhov's Reading, vol. 1959, 060001. AIP, Melville (2018)
2. Andries, P., Le Tallec, P., Perlat, J.-P., Perthame, B.: The Gaussian-BGK model of Boltzmann equation with small Prandtl number. Eur. J. Mech. B/Fluids **19**, 813–830 (2000)
3. Arima, T., Ruggeri, T., Sugiyama, M.: Rational extended thermodynamics of a rarefied polyatomic gas with molecular relaxation processes. Phys. Rev. E **96**, 042143 (2017)
4. Arima, T., Ruggeri, T., Sugiyama, M.: Extended thermodynamics of rarefied polyatomic gases: 15-field theory incorporating relaxation processes of molecular rotation and vibration. Entropy **20**, 301 (2018)
5. Arima, T., Ruggeri, T., Sugiyama, M., Taniguchi, S.: Non-linear extended thermodynamics of real gases with 6 fields. Int. J. Non-Linear Mech. **72**, 6–15 (2015)
6. Arima, T., Taniguchi, S., Ruggeri, T., Sugiyama, M.: Extended thermodynamics of real gases with dynamic pressure: an extension of Meixner's theory. Phys. Lett. A **376**, 2799–2803 (2012)
7. Baranger, C., Marois, G., Mathé, J., Mathiaud, J., Mieussens, L.: A BGK model for high temperature rarefied gas flows. (submitted)
8. Bird, G.A.: Molecular Gas Dynamics and the Direct Simulation of Gas Flows. Oxford University Press, Oxford (1994)
9. Bisi, M., Ruggeri, T., Spiga, G.: Dynamical pressure in a polyatomic gas: Interplay between kinetic theory and extended thermodynamics. Kin. Rel. Models **11**, 71–95 (2018)
10. Bisi, M., Spiga, G.: On kinetic models for polyatomic gases and their hydrodynamic limits. Ricerche Mat. **66**, 113–124 (2017)
11. Bourgat, J.-F., Desvillettes, L., Le Tallec, P., Perthame, B.: Microreversible collisions for polyatomic gases and Boltzmann's theorem. Eur. J. Mech. B/Fluids **13**, 237–254 (1994)
12. Boyd, I.D., Schwartzentruber, T.E.: Nonequilibrium Gas Dynamics and Molecular Simulation. Cambridge Univ. Press, Cambridge (2017)
13. Brau, C.A.: Kinetic theory of polyatomic gases: Models for the collision processes. Phys. Fluids **10**, 48–55 (1967)

14. Brull, S., Schneider, J.: On the ellipsoidal statistical model for polyatomic gases. Continuum Mech. Thermodyn. **20**, 489–508 (2009)
15. Cercignani, C.: The Boltzmann Equation and Its Applications. Springer, Berlin (1988)
16. Cercignani, C.: Rarefied Gas Dynamics: From Basic Concepts to Actual Calculations. Cambridge Univ. Press, Cambridge (2000)
17. Cercignani, C., Lampis, M.: On the H-theorem for polyatomic gases. J. Stat. Phys. **26**, 795–801 (1981)
18. Chapman, S., Cowling, T.G.: The Mathematical Theory of Non-uniform Gases, 3rd edition. Cambridge Univ. Press, Cambridge (1991)
19. Desvillettes, L., Monaco, R., Salvarani, F.: A kinetic model allowing to obtain the energy law of polytropic gases in the presence of chemical reactions. Eur. J. Mech. B/Fluids **24**, 219–236 (2005)
20. Ferziger, J.H., Kaper, H.G.: Mathematical Theory of Transport Processes in Gases. North Holland, Amsterdam (1972)
21. Gorji, M.H., Jenny, P.: A Fokker-Planck based kinetic model for diatomic rarefied gas flows. Phys. Fluids **25**, 062002 (2013)
22. Grad, H.: Principles of the kinetic theory of gases. In: Flügge, S. (ed.) Handbuch der Physik, Band XII, pp. 205–294. Springer, Berlin (1958)
23. Hanson, F.B., Morse, T.F.: Kinetic models for a gas with internal structure. Phys. Fluids **10**, 345–353 (1967)
24. Hattori, M., Kosuge, S., Aoki, K.: Slip boundary conditions for the compressible Navier–Stokes equations for a polyatomic gas. Phys. Rev. Fluids **3**, 063401 (2018)
25. Holway Jr., L.H.: New statistical models for kinetic theory: Methods of construction. Phys. Fluids **9**, 1658–1673 (1966)
26. Kogan, M.N.: Rarefied Gas Dynamics. Plenum, New York (1969)
27. Kosuge, S., Aoki, K.: Shock-wave structure for a polyatomic gas with large bulk viscosity. Phys. Rev. Fluids **3**, 023401 (2018)
28. Kosuge, S., Aoki, K., Goto, T.: Shock wave structure in polyatomic gases: Numerical analysis using a model Boltzmann equation. In: Ketsdever, A., Struchtrup, H. (eds.) AIP Conference Proceedings 30th International Symposium on Rarefied Gas Dynamics, vol. 1786, 180004. AIP, Melville (2016)
29. Kremer, G.M.: An Introduction to the Boltzmann Equation and Transport Processes in Gases. Springer, Berlin (2010)
30. Kustova, E.V., Nagnibeda, E.A., Shevelev, Yu.D., Syzranova, N.G.: Comparison of different models for non-equilibrium CO_2 flows in a shock layer near a blunt body. Shock Waves **21**, 273–287 (2011)
31. Liepmann, H.W., Roshko, A.: Elements of Gasdynamics. John Wiley & Sons, New York (1957)
32. Lin, J.T., Willis, D.R.: Kinetic theory analysis of temperature jump in a polyatomic gas. Phys. Fluids **15**, 31–38 (1972)
33. Liu, T.-P.: Hyperbolic conservation laws with relaxation. Commun. Math. Phys. **108**, 153–175 (1987)
34. Loyalka, S.K., Storvick, T.S.: Kinetic theory of thermal transpiration and mechanocaloric effect. III. Flow of a polyatomic gas between parallel plates. J. Chem. Phys. **71**, 339–350 (1979)
35. Mathiaud, J., Mieussens, L.: A Fokker-Planck model of the Boltzmann equation with correct Prandtl number. J. Stat. Phys. **162**, 397–414 (2016)
36. McCourt, F.R.W., Beenakker, J.J.M., Köhler, W.E., Kuščer, I.: Nonequilibrium Phenomena in Polyatomic Gases, Volume 1: Dilute Gases. Clarendon, Oxford (1990)
37. Morse, T.F.: Kinetic model for gases with internal degrees of freedom. Phys. Fluids **7**, 159–169 (1964)
38. Nagnibeda, E., Kustova, E.: Non-Equilibrium Reacting Gas Flows: Kinetic Theory of Transport and Relaxation Processes. Springer, Berlin (2009)
39. Nikitchenko, Yu.A.: Model kinetic equation for polyatomic gases. Comput. Math. and Math. Phys. **57**, 1843–1855 (2017)
40. Pavić-Čolić, M., Madjarević, D., Simić, S.: Polyatomic gases with dynamic pressure: Kinetic non-linear closure and the shock structure. Int. J. Non-Linear Mech. **92**, 160–175 (2017)
41. Rahimi, B., Struchtrup, H.: Capturing non-equilibrium phenomena in rarefied polyatomic gases: A high-order macroscopic model. Phys. Fluids **26**, 052001 (2014)

42. Rahimi, B., Struchtrup, H.: Macroscopic and kinetic modelling of rarefied polyatomic gases. J. Fluid Mech. **806**, 437–505 (2016)
43. Rossani, A., Spiga, G.: Kinetic theory with inelastic interactions. Transp. Theor. Stat. Phys. **27**, 273–287 (1998)
44. Ruggeri, T.: Non-linear maximum entropy principle for a polyatomic gas subject to the dynamic pressure. Bull. Inst. Math. Acad. Sinica (New Series) **11**, 1–22 (2016)
45. Ruggeri, T., Sugiyama, M.: Rational Extended Thermodynamics beyond the Monatomic Gas. Springer International Publishing Switzerland (2015)
46. Rykov, V.A.: A model kinetic equation for a gas with rotational degrees of freedom. Fluid Dyn. **10**, No. 6, 959–966 (1975)
47. Sharipov, F.: Data on the velocity slip and temperature jump on a gas-solid interface. J. Phys. Chem. Ref. Data **40**, 023101 (2011)
48. Sone, Y.: Molecular Gas Dynamics: Theory, Techniques, and Applications. Birkhäuser, Boston (2007)
49. Struchtrup, H.: The BGK model for an ideal gas with an internal degree of freedom. Transp. Theor. Stat. Phys. **28**, 369–385 (1999)
50. Takata, S., Funagane, H., Aoki, K.: Fluid modeling for the Knudsen compressor: Case of polyatomic gases. Kin. Rel. Models **3**, 353–372 (2010)
51. Taniguchi, S., Arima, T., Ruggeri, T., Sugiyama, M.: Effect of the dynamic pressure on the shock wave structure in a rarefied polyatomic gas. Phys. Fluids **26**, 016103 (2014)
52. Taniguchi, S., Arima, T., Ruggeri, T., Sugiyama, M.: Thermodynamic theory of the shock wave structure in a rarefied polyatomic gas: Beyond the Bethe-Teller theory. Phys. Rev. E **89**, 013025 (2014)
53. Taniguchi, S., Arima, T., Ruggeri, T., Sugiyama, M.: Overshoot of the non-equilibrium temperature in the shock wave structure of a rarefied polyatomic gas subject to the dynamic pressure. Int. J. Non-Linear Mech. **79**, 66–75 (2016)
54. Taniguchi, S., Arima, T., Ruggeri, T., Sugiyama, M.: Shock wave structure in rarefied polyatomic gases with large relaxation time for the dynamic pressure. IOP Conf. Series: J. Phys.: Conf. Series **1035**, 012009 (2018)
55. Willis, D.R., Hamel, B.B.: Non-equilibrium effects in spherical expansions of polyatomic gases and gas mixtures. In: Brundin, C.L. (ed.) Rarefied Gas Dynamics, vol. I, pp. 837–860. Academic Press, New York (1967)